Nonlinear Dyn (2019) 97:1175–1195
https://doi.org/10.1007/s11071-019-05039-w

ORIGINAL PAPER

# Primary and secondary resonance analyses of a cantilever beam carrying an intermediate lumped mass with time-delay feedback

**Chun-Xia Liu · Yan Yan · Wen-Quan Wang**

Received: 9 November 2018 / Accepted: 30 May 2019 / Published online: 25 June 2019


**Abstract** Time-delay displacement and velocity feedback of different types of active control in a cantilever beam carrying an lumped mass is investigated in this paper. Based on Euler–Bernoulli beam theory, the nonlinear governing equation is studied with damping, harmonic distribution, displacement delay, velocity delay and two time delays. The multiple scales perturbation method is applied to obtain the frequency response equations near primary, superharmonic and subharmonic resonances. A thorough study on the stability is proposed, with a particular emphasis on delay feedback. The results show that the hardening and softening behaviors of the system depend on the location of lumped mass. Furthermore, the displacement feedback gain coefficient only makes the peak amplitude move to the low frequency, yet velocity feedback coefficient and their time delays can be used to effectively enhance the stability and quench the nonlinear vibration of the cantilever beam. Thus, reasonable selection of the control system parameters can effectively improve the level of vibration control for the mechanical system.

C.-X. Liu · Y. Yan (✉) · W.-Q. Wang (✉)
Department of Engineering Mechanics, Kunming University of Science and Technology, Kunming 650500, Yunnan, People's Republic of China
e-mail: yanyankm@126.com

W.-Q. Wang
e-mail: wqwangkm@126.com

**Keywords** A cantilever beam · Time delay feedback · Multiple scales method · Subharmonic · Superharmonic

## 1 Introduction

The study of a cantilever beam with an intermediate lumped mass at an arbitrary position subjected to base excitation can find applications in robotic manipulators, components of high-speed machinery, structural buildings and many other structural elements [1–5]. If internal resonance is involved in such a system, the response and stability analysis will be more complicated. Therefore, the study of instability has attracted much attention in recent years [6–10]. For example, Nayfeh and Younis [11] studied the dynamics of electrically actuated microbeams under secondary, superharmonic and subharmonic resonances and found that a dynamic pull-in instability can occur at an electric load much lower than a pure DC voltage. Ekici and Boyaci [12] examined the nonlinear vibrations of microbeams using the multiple scales method and solved the equation of motion for two cases of subharmonic and superharmonic resonances. It was found that nonideal boundary conditions have a certain influence on the vibration of microbeams. Mehran et al. [13] studied the nonlinear forced vibration of a cantilever beam with an intermediate lumped mass and found that the frequency response of the cantilever beam is strongly influenced by the damping and excitation lev-

els. Eftekhari et al [14,15] investigated the dynamical behaviors of an aeroelastic panel and pointed out that for linear systems, a nonlinear feedback force should be used to obtain bifurcation boundary and produce limit cycle oscillation as the system response. Oveissi et al [16] and Toghraie et al [17] all studied the vibration and instability of axially moving carbon nanotubes conveying fluids and found that the stationary CNT conveying fluid is more stable than all cases of the axially moving CNT conveying fluid.

In addition to the study of a cantilever beam with an intermediate lumped mass, the control of various nonlinear systems [18–22] has been investigated recently. Because the flexibility of active control and time delay [23–27] are more common and unavoidable in controlled systems, many researchers are working on nonlinear systems with time delay. For example, Hu et al. [28] studied the resonance of a harmonic forced Duffing oscillator with time-delay feedback using a multiple scales method. They found that appropriate choices of the feedback gain coefficient and the time delay value enable better vibration control. Hu and Wang [29] considered the primary and subharmonic resonances of a harmonic forced Duffing oscillator with time delay and discussed the stability of periodic motion. In Refs. [30–37], the authors studied time-delay controllers and found that the time delay can be used as a control parameter to suppress the vibration of the dynamic system. Alhazza et al. [38–40] studied the nonlinear vibrations of a cantilever beam when excited externally and parametrically with linear and nonlinear time-delay feedback control. They found that time-delay control could feasibly reduce the system vibrations. Daqaq et al. [41] studied the nonlinear vibration of a piezoelectric-coupled cantilever beam by time-delay acceleration feedback control. They demonstrated that when the excitation frequency is very close to the least-damped delay frequency and the excitation amplitude is sufficiently large, the homogeneous solution emanating from the delayed feedback locks onto the particular solution resulting from the primary excitation.

Although many studies have been carried out on the stability of systems under time-delay control, to the best of the author's knowledge, a rigorous analysis of cantilever beams carrying a lumped mass has not been presented. In this paper, the nonlinear behavior of a cantilever beam carrying a lumped mass with both delayed displacement and velocity feedbacks is investigated. Based on Euler–Bernoulli beam theory, the nonlinear governing equation is studied with damping, harmonic distribution, displacement delay, velocity delay and two time delays. The primary and secondary resonances of this control system are determined using multiple scales analysis. All subharmonic and superharmonic conditions are obtained. The steady-state frequency response curves of the system in each case are given, and the amplitude-stable and unstable portions of the frequency response are determined. Then, comprehensive sensitivity studies are carried out for different time-delay parameters (displacement feedback gain coefficient, velocity feedback gain coefficient, displacement feedback and velocity feedback), and the effects of different parameters on the nonlinear system behavior are compared.

## 2 Mathematical model

In this section, a cantilever beam carrying an intermediate lumped mass is shown in Fig. 1. The cantilever beam with a length $l$ and a mass per unit length $m$ has a lumped mass located at a distance $d$ from its base. The cantilever beam is connected to a joint rotation spring of $K_r$ at the base and is subjected to a harmonic distribution load of amplitude $P$. We use the total kinetic and potential energy of the beam to obtain the corresponding Lagrangian:

$$L=\frac{ml}{2}\left[\begin{array}{l} c_1\left(\frac{\mathrm{d}u}{\mathrm{d}\tau}\right)^2+\frac{c_3u^2}{l^2}\left(\frac{\mathrm{d}u}{\mathrm{d}\tau}\right)^2+\frac{c_4u^2}{l^2}\left(\frac{\mathrm{d}u}{\mathrm{d}\tau}\right)^2 \\ +\frac{c_5u^4}{l^4}\left(\frac{\mathrm{d}u}{\mathrm{d}\tau}\right)^2+\frac{c_6u^4}{l^4}\left(\frac{\mathrm{d}u}{\mathrm{d}\tau}\right)^2 \\ -\left(\frac{EI}{ml^4}\right)\left(c_2u^2+\frac{c_7u^4}{l^2}+\frac{c_8u^6}{l^4}\right) \end{array}\right]$$

where $u(\tau)$ denotes the time dependence of the beam displacement. $E$ and $I$ represent the Young's modulus of elasticity and the moment of inertia, respectively.

The constant values $c_1-c_8$ are defined as follows:

$$c_1=\int_0^1\phi^2\mathrm{d}\varsigma+\rho\phi^2(\eta);\ c_2=\int_0^1\phi''^2\mathrm{d}\varsigma;$$

$$c_3=\int_0^1\left(\int_0^\varsigma\phi'^2\mathrm{d}\chi\right)^2\mathrm{d}\varsigma;$$

$$c_4=\rho\left[\left(\int_0^\varsigma\phi'^2\mathrm{d}\chi\right)^2\right]_{\varsigma=\eta};$$

$$c_5=\int_0^1\left[\left(\int_0^\varsigma\phi'^2\mathrm{d}\chi\right)\left(\int_0^\varsigma\phi'^4\mathrm{d}\chi\right)\right]\mathrm{d}\varsigma;$$

$$c_6=\rho\left[\left(\int_0^\varsigma\phi'^2\mathrm{d}\chi\right)\left(\int_0^\varsigma\phi'^4\mathrm{d}\chi\right)\right]_{\varsigma=\eta};$$

$$c_7=\int_0^1\phi'^2\phi''^2\mathrm{d}\varsigma;\ c_8=\int_0^1\phi'^4\phi''^2\mathrm{d}\varsigma$$

where $\phi(\varsigma)$ is the eigenfunction of the beam, which is written as [24] $\phi(\zeta)=\frac{\sin\beta\zeta-U\sinh\beta\zeta-V(\cos\beta\zeta-\cosh\beta\zeta)}{r}$

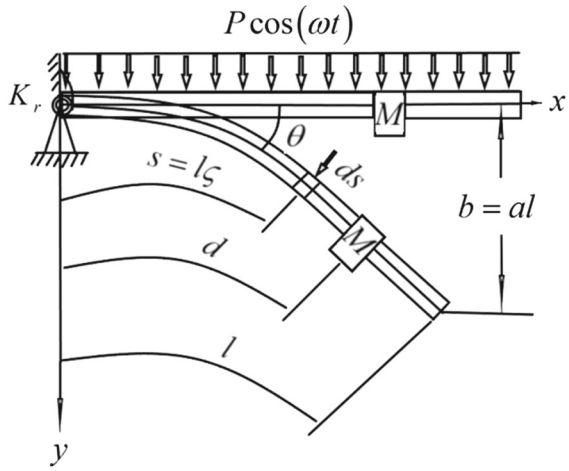


**Fig. 1** Schematic of a cantilever beam carrying a lumped mass under harmonic loading

Here, $r\,(r = \phi\,(1))$ is the scaling factor, $\beta$ is a dimensionless frequency parameter defined by $\beta^4 = \frac{m\omega_0^2 l^4}{EI}$, and $\omega_0$ is the natural frequency of the beam. $U$ and $V$ are, respectively, defined as $U = \frac{lK_r - 2EI\beta\sin\beta(\cos\beta+\cosh\beta)}{lK_r + 2EI\beta\sinh\beta(\cos\beta+\cosh\beta)}$, $V = \frac{\sin\beta + U\sinh\beta}{\cos\beta+\cosh\beta}$.

The dimensionless parameters $\eta = \frac{d}{l}$, $\varsigma = \frac{s}{l}$, $\rho = \frac{M}{ml}$ represent the distance, span length and mass ratio, respectively. $\rho$ is the mass density per unit length.

By employing the Euler-Lagrange equation, the dimensionless governing equation of motion for the dynamics is as follows [17]:

$$\ddot{u} + u + \mu\dot{u} + \alpha_1 u^3 + \alpha_2 u^5 + \beta_1 u^2\ddot{u} + \beta_1 u\dot{u}^2 + \beta_2 u^4\ddot{u} + \beta_2 u^3\dot{u}^2 = F\cos(\Omega t) \tag{1}$$

where $\mu$ is the damping coefficient. The coefficients $\alpha_1$, $\alpha_2$, $\beta_1$ and $\beta_2$ are defined as $\alpha_1 = \frac{2c_7}{c_2}$, $\alpha_2 = \frac{2c_8}{c_2}$, $\beta_1 = \frac{c_3c_4}{\beta^4 c_1}$, $\beta_2 = \frac{c_5c_6}{\beta^4 c_1}$. $t = \tau\sqrt{\frac{EIc_2}{l^4c_1m}}$, $F = \frac{P}{\int_0^1 \phi^2 \mathrm{d}\varsigma}$, and $\Omega = \frac{\omega}{\omega_0}$ is the dimensionless excitation frequency.

By integrating the time-delayed displacement and velocity feedback controller into system (1), Eq. (2) becomes the following:

$$\ddot{u} + u + \mu\dot{u} + \alpha_1 u^3 + \alpha_2 u^5 + \beta_1 u^2\ddot{u} + \beta_1 u\dot{u}^2 + \beta_2 u^4\ddot{u} + \beta_2 u^3\dot{u}^2 = F\cos(\Omega t) + g_p u(t-\tau_1) + g_d\dot{u}(t-\tau_2) \tag{2}$$

where $g_p$, $g_d$, $\tau_1$ and $\tau_2$ are the displacement feedback coefficient, velocity feedback coefficient and time delays of the displacement and velocity feedbacks, respectively.

## 3 Multiple scales method

### 3.1 Primary resonance

In this section, we use the multiple scales method to obtain an accurate analytical solution of a cantilever beam. To obtain the primary resonance of the system, supposing a small perturbation parameter $\varepsilon$, Eq. (2) can be rewritten as follows:

$$\ddot{u} + u = \varepsilon\begin{pmatrix} -\mu\dot{u} - \alpha_1 u^3 - \alpha_2 u^5 - \beta_1 u^2\ddot{u} \\ -\beta_1 u\dot{u}^2 - \beta_2 u^4\ddot{u} + \beta_2 u^3\dot{u}^2 \\ +F\cos(\Omega t) + g_p u(t-\tau_1) \\ +g_d\dot{u}(t-\tau_2) \end{pmatrix} \tag{3}$$

We assume that the frequency of the actuation is close to the fundamental frequency:

$$\Omega = 1 + \varepsilon\sigma \tag{4}$$

where $\sigma$ is the nonlinear detuning parameter. Let $T_n = \varepsilon^n t$, $(n = 0,\ 1,\ 2)$ and the displacement be $u_0(t) = u_0(T_0, T_1, T_2)$. Equation (3) can be expanded Eqs. (5) and (6):

$$u(t) = u_0(T_0, T_1, T_2) + \varepsilon u_1(T_0, T_1, T_2) + \varepsilon^2 u_2(T_0, T_1, T_2)\cdots \tag{5}$$

$$u(t-\tau_i) = u_0(T_0 - \tau_i, T_1 - \varepsilon\tau_i, T_2 - \varepsilon^2\tau_i) + \varepsilon u_1(T_0 - \tau_i, T_1 - \varepsilon\tau_i, T_2 - \varepsilon^2\tau_i) + \varepsilon^2 u_2(T_0 - \tau_i, T_1 - \varepsilon\tau_i, T_2 - \varepsilon^2\tau_i)\cdots, \quad i = 1, 2 \tag{6}$$

The time derivatives are defined as follows:

$$\frac{d}{dt} = D_0 + \varepsilon D_1 + \varepsilon^2 D_2 + \cdots \tag{7}$$

$$\frac{d^2}{dt^2} = D_0^2 + 2\varepsilon D_0 D_1 + \varepsilon^2\left(D_1^2 + 2D_0 D_2\right) + \cdots \tag{8}$$

By substituting Eqs. (5-8) into Eq. (3) and equating the coefficients of $\varepsilon$, we have

$$\varepsilon^0:\ D_0^2 u_0 + u_0 = 0 \tag{9}$$

$$\varepsilon^1:\ D_0^2 u_1 + u_1 = -\mu D_0 u_0 - 2D_0 D_1 u_0 - \alpha_1 u_0^3 - \alpha_2 u_0^5 - \beta_1 u_0^2 D_0^2 u_0 - \beta_1 u_0 (D_0 u_0)^2 - \beta_2 u_0^4\left(D_0^2 u_0\right) - \beta_2 u_0^3 (D_0 u_0)^2 + g_p u_{0\tau_1} + g_d D_0 u_{0\tau_2} + F\cos(\Omega t) \tag{10}$$

The general solution of Eq. (9) is

$$u_0 = A(T_1, T_2)e^{iT_0} + \bar{A}(T_1, T_2)e^{-iT_0} \tag{11a}$$

and

$$u_{0\tau_i} = A(T_1 - \varepsilon\tau_1, T_2 - \varepsilon^2\tau_2)e^{i(T_0-\tau_i)} + \bar{A}(T_1 - \varepsilon\tau_1, T_2 - \varepsilon^2\tau_{22})e^{-i(T_0-\tau_i)} \tag{11b}$$

where $A$ and $\bar{A}$ are the complex amplitude and complex conjugate of $A$, respectively.

Given the fact that $\varepsilon$ is very small compared to unity, after expansion by Taylor's

formula, we get

$$\begin{aligned} &A(T_1 - \varepsilon\tau_1, T_2 - \varepsilon^2\tau_2) \\ &= A(T_1, T_2) - \varepsilon\tau_j D_1 A(T_1, T_2) \\ &\quad -\varepsilon^2\tau_j D_2 A(T_1, T_2) + \cdots \cong A(T_1, T_2) \end{aligned} \tag{12}$$

Substituting Eqs. (11, 12) into Eq. (10),

$$\begin{aligned} &D_0^2 u_1 + \omega_0^2 u_1 \\ &= \frac{1}{2}Fe^{i\Omega T_0} - \alpha_1 A^3 e^{3iT_0} \\ &\quad - \alpha_2 A^5 e^{5iT_0} - 5\alpha_2 A^4 \bar{A} e^{3iT_0} \\ &\quad + 2\beta_1 A^3 e^{3iT_0} + 2\beta_2 A^5 e^{5iT_0} + 6\beta_2 A^4 \bar{A} e^{3iT_0} \\ &\quad + \begin{pmatrix} -3\alpha_1 A^2\bar{A} - 10\alpha_2 A^3\bar{A}^2 - i\mu A + 2\beta_1 A^2\bar{A} \\ +8\beta_2 A^3\bar{A}^2 - 2i\dot{A} \\ +g_p A e^{-i\tau_1} + ig_d A e^{-i\tau_2} \end{pmatrix} e^{iT_0} \\ &\quad + c.c \end{aligned} \tag{13}$$

where $c.c$ represents the complex conjugate of all terms.

Eliminating the secular term in Eq. (13), the following expression is obtained:

$$\begin{aligned} &-3\alpha_1 A^2\bar{A} - 10\alpha_2 A^3\bar{A}^2 - i\mu A + 2\beta_1 A^2\bar{A} \\ &\quad + 8\beta_2 A^3\bar{A}^2 - 2i\dot{A} + \frac{1}{2}Fe^{i\sigma T_1} + g_p A e^{-i\tau_1} \\ &\quad + ig_d A e^{-i\tau_2} = 0 \end{aligned} \tag{14}$$

By assuming $A = \frac{ae^{i\theta}}{2}$, substituting it into Eq. (14), and separating the real and imaginary parts, we have the result

$$\dot{a} = -\frac{\mu a}{2} + \frac{F}{2}\sin\gamma - \frac{ag_p}{2}\sin(\tau_1) + \frac{ag_d}{2}\cos(\tau_2) \tag{15}$$

$$a\dot{\gamma} = a\sigma + \frac{F}{2}\cos\gamma - \frac{3\alpha_1 a^3}{8} - \frac{5\alpha_2 a^5}{16} + \frac{\beta_1 a^3}{4} + \frac{\beta_2 a^5}{4} + \frac{ag_p}{2}\cos(\tau_1) + \frac{ag_d}{2}\sin(\tau_2) \tag{16}$$

where $\gamma = \sigma T_1 - \theta$.

Letting $\dot{a} = a\dot{\gamma} = 0$, we obtain the frequency response equation

$$\begin{aligned} \frac{F^2}{4} &= \left(\frac{\mu a}{2} + \frac{ag_p}{2}\sin(\tau_1) - \frac{ag_d}{2}\cos(\tau_2)\right)^2 \\ &\quad + \left(a\sigma - \frac{3\alpha_1 a^3}{8} - \frac{5\alpha_2 a^5}{16} + \frac{\beta_1 a^3}{4} + \frac{\beta_2 a^5}{4} \right. \\ &\quad \left. + \frac{ag_p}{2}\cos(\tau_1) + \frac{ag_d}{2}\sin(\tau_2)\right)^2 \end{aligned} \tag{17}$$

The peak value of the primary resonance can be obtained by Eq. (17)

$$a_{\max} = \frac{F}{2\mu_0} \tag{18}$$

here $\mu_0 = \frac{\mu + g_p\sin\tau_1 - g_d\cos\tau_2}{2}$.

The corresponding peak amplitude of uncontrolled system is

$$\bar{a}_{\max} = \frac{F}{\mu} \tag{19}$$

Since the analytical solution of the nonlinear vibration system is usually difficult to solve, the study of the time-delay control performance of the nonlinear vibration system cannot simply adopt the form of the response amplitude ratio similar to the linear vibration system. Therefore, the attenuation ratio of the peak amplitude of primary resonance response, denoted by R, is defined by the ratio of the peak amplitude of primary resonance vibrations with and without the attachment. The vibration control performance is evaluated by using the attenuation rate [42]. The attenuation ratio is expressed as follows:

$$R = \frac{a_{\max}}{\bar{a}_{\max}} = \frac{1}{1 + \frac{g_p\sin\tau_1 - g_d\cos\tau_2}{\mu}} \tag{20}$$

As can be seen from Eq. (20) that a small value of $R$ indicates a large reduction in amplitude which indicates that the level of vibration control is effectively improved. A smaller attenuation rate can be obtained by selecting an appropriate feedback gain factors and time delays.

For simplicity, two delays are expressed as $\tau_1 = \tau$ and $\tau_2 = \phi + \tau$. As the phase of velocity is ahead of displacement by $\frac{\pi}{2}$, the phase difference $\phi$ can be assumed as $\frac{\pi}{2}$ [43]. Equation (20) can be rewritten as

$$R = \frac{1}{1 + \frac{(g_p + g_d)\sin\tau}{\mu}} \tag{21}$$

The stability of solutions is determined by the eigenvalues of the corresponding Jacobian matrix of Eqs. 15 and

16. The eigenvalue is the root of the following equation

$$\lambda^2 + 2\mu_0\lambda + \mu_0^2 + \left(\sigma_0 - v_0a^2 - v_1a^4\right) \left(\sigma_0 - 3v_0a^2 - 5v_1a^4\right) = 0 \tag{22}$$

The sufficient condition of system stability is

$$f(\sigma_0) = \mu_0^2 + \left(\sigma_0 - v_0a^2 - v_1a^4\right) \left(\sigma_0 - 3v_0a^2 - 5v_1a^4\right) > 0, \quad \mu_0 > 0 \tag{23}$$

When the critical equation $f(\sigma_0) = 0$ has no real solution, the value of $f(\sigma_0)$ is always positive. Then, the expression is as

$$\begin{aligned}\mu_0^2 &\geq v_0^2a_{\max}^4 + 4v_0v_1a_{\max}^6 + 4v_1^2a_{\max}^8 \\ &\geq v_0^2a^4 + 4v_0v_1a^6 + 4v_1^2a^8\end{aligned} \tag{24}$$

where $v_0 = \frac{3\alpha_1}{8} - \frac{\beta_1}{4}$, $v_1 = \frac{5\alpha_2}{16} - \frac{\beta_2}{4}$.

Substituting Eq. (18) into Eq. (24), the region of the stable vibration control parameters is satisfied as

$$(\mu + g_{\tau 1}\sin\tau)^{10} \geq 4v_0^2F^4(\mu + g_{\tau 1}\sin\tau)^4 + 16v_0v_1F^6(\mu + g_{\tau 1}\sin\tau)^2 + 16v_1^2F^8, \mu_0 > 0 \tag{25}$$

When the critical equation $f(\sigma_0) = 0$ has two real solutions, the stable vibration region is

$$g_{\tau 2}\cos\tau \geq \frac{8v_0F^2\mu^2 + 3v_1F^4 + 2\sqrt{4v_0^2F^4\mu^4 + 4v_0v_1F^6\mu^2 + v_1^2F^8 - \mu^{10}}}{8\mu^4} - 2\sigma, \quad \mu_0 > 0 \tag{26}$$

or

$$g_{\tau 3}\cos\tau \leq -\frac{\sqrt{4v_0^2F^4\mu^4 + 4v_0v_1F^6\mu^2 + v_1^2F^8 - \mu^{10}}}{4\mu^4} - 2\sigma, \quad \mu_0 > 0 \tag{27}$$

where $g_{\tau i} = \left(g_p + g_d\right)$, $i = 1, 2, 3$.

In a word, if the critical equation has no real solution, the optimal design of the control parameters meets $\min \frac{1}{1+\frac{g_{\tau 1}\sin\tau}{\mu}}$ and Eq. (25). If the critical equation has two real solution, the optimal design of the control parameters satisfies $\min \frac{1}{1+\frac{(g_p+g_d)\sin\tau}{\mu}}$ and Eq. (26), or $\min \frac{1}{1+\frac{(g_p+g_d)\sin\tau}{\mu}}$ and Eq. (27).

Obviously, when nonlinear control parameters, excitation amplitude, damping coefficient, time delays and natural frequency of the system are known, feedback gain coefficients, attenuation ratio and also the optimal time delays can be obtained.

### 3.2 Secondary resonance

To investigate the superharmonic and subharmonic resonances of a cantilever beam with time delay, Eq. (2) can be rewritten as follows:

$$\ddot{u} + u = \varepsilon\begin{pmatrix} -\mu\dot{u} - \alpha_1u^3 - \alpha_2u^5 - \beta_1u^2\ddot{u} - \beta_1u\dot{u}^2 \\ -\beta_2u^4\ddot{u} - \beta_2u^3\dot{u}^2 \\ +g_pu(t-\tau_1) + g_d\dot{u}(t-\tau_2)\end{pmatrix} + F\cos(\Omega t) \tag{28}$$

By substituting Eqs. (5)–(8) into Eq. (28) and equating the coefficients of ε, we have

$$\varepsilon^0: \ D_0^2u_0 + u_0 = F\cos(\Omega t) \tag{29}$$

$$\begin{aligned}\varepsilon^1: \ D_0^2u_1 + u_1 = &-\mu D_0u_0 - 2D_0D_1u_0 - \alpha_1u_0^3 \\ &-\alpha_2u_0^5 - \beta_1u_0^2D_0^2u_0 - \beta_1u_0(D_0u_0)^2 \\ &-\beta_2u_0^4\left(D_0^2u_0\right) - \beta_2u_0^3(D_0u_0)^2 \\ &+g_pu_{0\tau_1} + g_dD_0u_{0\tau_2}\end{aligned} \tag{30}$$

The general solution of Eq. (22) is

$$u_0 = A(T_1, T_2)e^{iT_0} + \Lambda(T_1, T_2)e^{i\Omega T_0} + c.c \tag{31}$$

where $\Lambda = \frac{F}{2(1-\Omega^2)}$.

Substituting Eq. (31) into (30), we obtain Eq. (32), which is presented in Appendix A. All the conditions of the secondary resonances of the control system (2) can be recognized, and the corresponding amplitude–frequency response equation is studied in the next section.

#### *3.2.1 Superharmonic resonances of $\omega \approx \frac{1}{2}\omega_0$, $\omega \approx \frac{1}{3}\omega_0$ and $\omega \approx \frac{1}{5}\omega_0$*

Here, we assume that the frequency of actuation is close to one-half of the fundamental frequency:

$$2\Omega = 1 + \varepsilon\sigma \tag{33}$$

Substituting Eq. (33) into Eq. (32), the secular terms are collected, and then, we have

$$\begin{aligned}&-6A\Lambda^2\alpha_1 - 3A^2\bar{A}\alpha_1 - 30A\Lambda^4\alpha_2 - 60A^2\Lambda^2\bar{A}\alpha_2 \\ &-10A^3\bar{A}^2\alpha_2 + 2A\Lambda^2\Omega^2\beta_1 \\ &+18A\Lambda^4\Omega^2\beta_2 + 18A^2\Lambda^2\bar{A}\Omega^2\beta_2 - i\mu A \\ &+2A\Lambda^2\beta_1 + 2A^2\bar{A}\beta_1 + 6A\Lambda^4\beta_2 \\ &+30A^2\Lambda^2\bar{A}\beta_2 + 8A^3\bar{A}^2\beta_2 \\ &+e^{2i\sigma T_1}\left(-5\Lambda^4\bar{A}\alpha_2 + 7\Lambda^4\bar{A}\Omega^2\beta_2\right.\end{aligned}$$

$$-2\Lambda^4\bar{A}\Omega\beta_2+\Lambda^4\bar{A}\beta_2\Big)$$
$$-2i\dot{A}+g_pAe^{-i\tau_1}+ig_dAe^{-i\tau_2}=0 \tag{34}$$

By assuming $A=\frac{ae^{i\theta}}{2}$ and separating the real and imaginary parts, the frequency response equation of the steady-state solutions is obtained

$$\left(-\frac{5a\Lambda^4\alpha_2}{2}+\frac{7a\Lambda^4\Omega^2\beta_2}{2}-a\Lambda^4\Omega\beta_2+\frac{a\Lambda^4\beta_2}{2}\right)^2$$
$$=\left(\frac{\mu a}{2}+\frac{ag_p\sin\tau_1}{2}-\frac{ag_d\cos\tau_2}{2}\right)^2$$
$$+\begin{pmatrix}a\sigma-3a\Lambda^2\alpha_1-\frac{3a^3\alpha_1}{8}-15a\Lambda^4\alpha_2\\-\frac{15a^3\Lambda^2\alpha_2}{2}-\frac{5a^5\alpha_2}{16}+a\Lambda^2\Omega^2\beta_1\\+9a\Lambda^4\Omega^2\beta_2+\frac{9a^3\Lambda^2\Omega^2\beta_2}{4}+a\Lambda^2\beta_1\\+\frac{a^3\beta_1}{4}+3a\Lambda^4\beta_2+\frac{15a^3\Lambda^2\beta_2}{4}+\frac{a^5\beta_2}{4}\\+\frac{ag_p\cos\tau_1}{2}+\frac{ag_d\sin\tau_2}{2}\end{pmatrix}^2 \tag{35}$$

Similarly, when $3\Omega=1+\varepsilon\sigma$ is substituted into Eq. (32), one obtains

$$\begin{aligned}&-6A\Lambda^2\alpha_1-3A^2\bar{A}\alpha_1-30A\Lambda^4\alpha_2-60A^2\Lambda^2\bar{A}\alpha_2\\&-10A^3\bar{A}^2\alpha_2+2A\Lambda^2\Omega^2\beta_1\\&+18A\Lambda^4\Omega^2\beta_2+18A^2\Lambda^2\bar{A}\Omega^2\beta_2-i\mu A\\&+2A\Lambda^2\beta_1+2A^2\bar{A}\beta_1+6A\Lambda^4\beta_2\\&+30A^2\Lambda^2\bar{A}\beta_2+8A^3\bar{A}^2\beta_2\\&+e^{i\sigma T_1}\begin{pmatrix}-\Lambda^3\alpha_1-5\Lambda^5\alpha_2-20A\Lambda^3\bar{A}\alpha_2+2\Lambda^3\Omega^2\beta_1\\+6\Lambda^5\Omega^2\beta_2+18A\Lambda^3\bar{A}\Omega^2\beta_2+6A\Lambda^3\bar{A}\beta_2\end{pmatrix}\\&+e^{-i\sigma T_1}\Big(-10A^2\Lambda^3\alpha_2+9A^2\Lambda^3\Omega^2\beta_2\\&-6A^2\Lambda^3\Omega\beta_2+5A^2\Lambda^3\beta_2\Big)\\&-2i\dot{A}+g_pAe^{-i\tau_1}+ig_dAe^{-i\tau_2}=0\end{aligned} \tag{36}$$

Similarly, the frequency response equation of the steady-state solutions is obtained:

$$\begin{pmatrix}-\Lambda^3\alpha_1-5\Lambda^5\alpha_2-\frac{5a^2\Lambda^3\alpha_2}{2}\\+2\Lambda^3\Omega^2\beta_1+6\Lambda^5\Omega^2\beta_1+\frac{9a^2\Lambda^3\Omega^2\beta_2}{4}\\+\frac{a^2\Lambda^3\beta_2}{4}-\frac{3a^2\Lambda^3\Omega\beta_2}{2}\end{pmatrix}^2\cdot$$
$$\begin{pmatrix}-\Lambda^3\alpha_1-5\Lambda^5\alpha_2-\frac{15a^2\Lambda^3\alpha_2}{2}\\+2\Lambda^3\Omega^2\beta_1+6\Lambda^5\Omega^2\beta_1+\frac{27a^2\Lambda^3\Omega^2\beta_2}{4}\\+\frac{11a^2\Lambda^3\beta_2}{4}-\frac{3a^2\Lambda^3\Omega\beta_2}{2}\end{pmatrix}^2$$
$$=\left(\frac{\mu a}{2}+\frac{ag_p\sin\tau_1}{2}-\frac{ag_d\cos\tau_2}{2}\right)^2$$
$$\begin{pmatrix}-\Lambda^3\alpha_1-5\Lambda^5\alpha_2-\frac{15a^2\Lambda^3\alpha_2}{2}\\+2\Lambda^3\Omega^2\beta_1+6\Lambda^5\Omega^2\beta_1+\frac{27a^2\Lambda^3\Omega^2\beta_2}{4}\\+\frac{11a^2\Lambda^3\beta_2}{4}-\frac{3a^2\Lambda^3\Omega\beta_2}{2}\end{pmatrix}^2$$
$$+\begin{pmatrix}a\sigma-3a\Lambda^2\alpha_1-\frac{3a^3\alpha_1}{8}-15a\Lambda^4\alpha_2\\-\frac{15a^3\Lambda^2\alpha_2}{2}-\frac{5a^5\alpha_2}{16}+a\Lambda^2\Omega^2\beta_1\\+9a\Lambda^4\Omega^2\beta_2+\frac{9a^3\Lambda^2\Omega^2\beta_2}{4}+a\Lambda^2\beta_1\\+\frac{a^3\beta_1}{4}+3a\Lambda^4\beta_2+\frac{15a^3\Lambda^2\beta_2}{4}+\frac{a^5\beta_2}{4}\\+\frac{ag_p\cos\tau_1}{2}+\frac{ag_d\sin\tau_2}{2}\end{pmatrix}^2$$
$$\begin{pmatrix}-\Lambda^3\alpha_1-5\Lambda^5\alpha_2-\frac{5a^2\Lambda^3\alpha_2}{2}\\+2\Lambda^3\Omega^2\beta_1+6\Lambda^5\Omega^2\beta_1\\+\frac{9a^2\Lambda^3\Omega^2\beta_2}{4}+\frac{a^2\Lambda^3\beta_2}{4}\\-\frac{3a^2\Lambda^3\Omega\beta_2}{2}\end{pmatrix}^2 \tag{37}$$

When $5\Omega=1+\varepsilon\sigma$, one obtains

$$\begin{aligned}&-6A\Lambda^2\alpha_1-3A^2\bar{A}\alpha_1-30A\Lambda^4\alpha_2-60A^2\Lambda^2\bar{A}\alpha_2\\&-10A^3\bar{A}^2\alpha_2+2A\Lambda^2\Omega^2\beta_1\\&+18A\Lambda^4\Omega^2\beta_2+18A^2\Lambda^2\bar{A}\Omega^2\beta_2-i\mu A\\&+2A\Lambda^2\beta_1+2A^2\bar{A}\beta_1+6A\Lambda^4\beta_2\\&+30A^2\Lambda^2\bar{A}\beta_2+8A^3\bar{A}^2\beta_2\\&+e^{i\sigma T_1}\Big(-\Lambda^5\alpha_2+2\Lambda^5\Omega^2\beta_2\Big)\\&-2i\dot{A}+g_pAe^{-i\tau_1}+ig_dAe^{-i\tau_2}=0\end{aligned} \tag{38}$$

Then, the steady-state responses of the system are:

$$\Big(-\Lambda^5\alpha_2+2\Lambda^5\Omega^2\beta_2\Big)^2=$$
$$\left(\frac{\mu a}{2}+\frac{ag_p\sin\tau_1}{2}-\frac{ag_d\cos\tau_2}{2}\right)^2$$
$$+\begin{pmatrix}a\sigma-3a\Lambda^2\alpha_1-\frac{3a^3\alpha_1}{8}-15a\Lambda^4\alpha_2\\-\frac{15a^3\Lambda^2\alpha_2}{2}-\frac{5a^5\alpha_2}{16}+a\Lambda^2\Omega^2\beta_1\\+9a\Lambda^4\Omega^2\beta_2+\frac{9a^3\Lambda^2\Omega^2\beta_2}{4}+a\Lambda^2\beta_1\\+\frac{a^3\beta_1}{4}+3a\Lambda^4\beta_2+\frac{15a^3\Lambda^2\beta_2}{4}+\frac{a^5\beta_2}{4}\\+\frac{ag_p\cos\tau_1}{2}+\frac{ag_d\sin\tau_2}{2}\end{pmatrix}^2 \tag{39}$$

### 3.2.2 *Subharmonic resonances of $\omega\approx 2\omega_0$, $\omega\approx 3\omega_0$ and $\omega\approx 5\omega_0$*

In this section, three cases of subharmonic resonances are studied.

Case 1: when $\Omega = 2 + \varepsilon\sigma$, one obtains

$$
\begin{aligned}
&-6A\Lambda^2\alpha_1 - 3A^2\bar{A}\alpha_1 - 30A\Lambda^4\alpha_2 - 60A^2\Lambda^2\bar{A}\alpha_2 \\
&-10A^3\bar{A}^2\alpha_2 + 2A\Lambda^2\Omega^2\beta_1 \\
&+18A\Lambda^4\Omega^2\beta_2 + 18A^2\Lambda^2\bar{A}\Omega^2\beta_2 - i\mu A \\
&+2A\Lambda^2\beta_1 + 2A^2\bar{A}\beta_1 + 6A\Lambda^4\beta_2 \\
&+30A^2\Lambda^2\bar{A}\beta_2 + 8A^3\bar{A}^2\beta_2 \\
&+e^{2i\sigma T_1}\begin{pmatrix} -10\Lambda^2\bar{A}^3\alpha_2 + 5\Lambda^2\bar{A}^3\Omega^2\beta_2 - 6\Lambda^2\bar{A}^3\beta_2 \\ +9\Lambda^2\bar{A}^3\beta_2 \end{pmatrix} \\
&-2i\dot{A} + g_p A e^{-i\tau_1} + ig_d A e^{-i\tau_2} = 0
\end{aligned} \tag{40}
$$

Then, the frequency response equation of the steady-state solutions is obtained:

$$
\begin{aligned}
&\left(-\frac{5a^3\Lambda^2\alpha_2}{4} + \frac{5a^3\Lambda^2\Omega^2\beta_2}{8} - \frac{3a^3\Lambda^2\beta_2}{4} + \frac{9a^3\Lambda^2\beta_2}{8}\right)^2 \\
&= \left(\frac{\mu a}{2} + \frac{ag_p\sin\tau_1}{2} - \frac{ag_d\cos\tau_2}{2}\right)^2 \\
&\quad + \begin{pmatrix} \frac{a\sigma}{2} - 3a\Lambda^2\alpha_1 - \frac{3a^3\alpha_1}{8} - 15a\Lambda^4\alpha_2 \\ -\frac{15a^3\Lambda^2\alpha_2}{2} - \frac{5a^5\alpha_2}{16} + a\Lambda^2\Omega^2\beta_1 \\ +9a\Lambda^4\Omega^2\beta_2 + \frac{9a^3\Lambda^2\Omega^2\beta_2}{4} + a\Lambda^2\beta_1 \\ +\frac{a^3\beta_1}{4} + 3a\Lambda^4\beta_2 + \frac{15a^3\Lambda^2\beta_2}{4} + \frac{a^5\beta_2}{4} \\ +\frac{ag_p\cos\tau_1}{2} + \frac{ag_d\sin\tau_2}{2} \end{pmatrix}^2
\end{aligned} \tag{41}
$$

Case 2: when $\Omega = 3 + \varepsilon\sigma$, one obtains

$$
\begin{aligned}
&-6A\Lambda^2\alpha_1 - 3A^2\bar{A}\alpha_1 - 30A\Lambda^4\alpha_2 - 60A^2\Lambda^2\bar{A}\alpha_2 \\
&-10A^3\bar{A}^2\alpha_2 + 2A\Lambda^2\Omega^2\beta_1 \\
&+18A\Lambda^4\Omega^2\beta_2 + 18A^2\Lambda^2\bar{A}\Omega^2\beta_2 - i\mu A \\
&+2A\Lambda^2\beta_1 + 2A^2\bar{A}\beta_1 + 6A\Lambda^4\beta_2 \\
&+30A^2\Lambda^2\bar{A}\beta_2 + 8A^3\bar{A}^2\beta_2 + e^{i\sigma T_1} \\
&\quad \begin{pmatrix} -3\Lambda\bar{A}^2\alpha_1 - 30\Lambda^3\bar{A}^2\alpha_2 - 20A\Lambda\bar{A}^3\alpha_2 \\ +\bar{A}^2\Lambda\Omega^2\beta_1 + 15\Lambda^3\Omega^2\bar{A}^2\beta_2 + 4A\Lambda\bar{A}^3\Omega^2\beta_2 \\ -2\Lambda\Omega\bar{A}^2\beta_1 - 6\Lambda^3\Omega\bar{A}^2\beta_2 - 4A\Lambda\bar{A}^3\Omega\beta_2 \\ +3\Lambda\bar{A}^2\beta_1 + 15\Lambda^3\bar{A}^2\beta_2 + 16A\Lambda\bar{A}^3\beta_2 \end{pmatrix} \\
&+e^{-i\sigma T_1}\left(-5A^4\Lambda\alpha_2 + A^4\Lambda\Omega^2\beta_2\right. \\
&\left.-2A^4\Lambda\Omega\beta_2 + 7A^4\Lambda\beta_2\right) \\
&-2i\dot{A} + g_p A e^{-i\tau_1} + ig_d A e^{-i\tau_2} = 0
\end{aligned} \tag{42}
$$

and the amplitude-frequency curve equation is

$$
\begin{aligned}
&\begin{pmatrix} -\frac{3\Lambda a^2\alpha_1}{4} - \frac{15\Lambda^3 a^2\alpha_2}{2} - \frac{15\Lambda a^4\alpha_2}{16} + \frac{\Lambda a^2\Omega^2\beta_1}{4} \\ +\frac{15\Lambda^3 a^2\Omega^2\beta_2}{4} + \frac{3\Lambda a^4\Omega^2\beta_2}{16} - \frac{\Lambda a^2\Omega\beta_1}{2} - \frac{3\Lambda^3 a^2\Omega\beta_2}{2} \\ -\frac{\Lambda a^4\Omega\beta_2}{8} + \frac{3\Lambda a^2\beta_1}{4} + \frac{15\Lambda^3 a^2\beta_2}{4} + \frac{9\Lambda a^4\beta_2}{16} \end{pmatrix}^2 \\
&\left(-\frac{3\Lambda a^2\alpha_1}{4} - \frac{15\Lambda^3 a^2\alpha_2}{2} - \frac{25\Lambda a^4\alpha_2}{16} + \frac{\Lambda a^2\Omega^2\beta_1}{4}\right. \\
&+\frac{15\Lambda^3 a^2\Omega^2\beta_2}{4} + \frac{5\Lambda a^4\Omega^2\beta_2}{16} - \frac{\Lambda a^2\Omega\beta_1}{2} - \frac{3\Lambda^3 a^2\Omega\beta_2}{2} \\
&\left.-\frac{3\Lambda a^4\Omega\beta_2}{8} + \frac{3\Lambda a^2\beta_1}{4} + \frac{15\Lambda^3 a^2\beta_2}{4} + \frac{23\Lambda a^4\beta_2}{16}\right)^2 \\
&= \left(\frac{\mu a}{2} + \frac{ag_p\sin\tau_1}{2} - \frac{ag_d\cos\tau_2}{2}\right)^2 \\
&\quad \begin{pmatrix} -\frac{3\Lambda a^2\alpha_1}{4} - \frac{15\Lambda^3 a^2\alpha_2}{2} - \frac{25\Lambda a^4\alpha_2}{16} \\ +\frac{\Lambda a^2\Omega^2\beta_1}{4} + \frac{15\Lambda^3 a^2\Omega^2\beta_2}{4} + \frac{5\Lambda a^4\Omega^2\beta_2}{16} \\ -\frac{\Lambda a^2\Omega\beta_1}{2} - \frac{3\Lambda^3 a^2\Omega\beta_2}{2} - \frac{3\Lambda a^4\Omega\beta_2}{8} \\ +\frac{3\Lambda a^2\beta_1}{4} + \frac{15\Lambda^3 a^2\beta_2}{4} + \frac{23\Lambda a^4\beta_2}{16} \end{pmatrix}^2 \\
&+ \begin{pmatrix} \frac{a\sigma}{3} - 3a\Lambda^2\alpha_1 - \frac{3a^3\alpha_1}{8} - 15a\Lambda^4\alpha_2 \\ -\frac{15a^3\Lambda^2\alpha_2}{2} - \frac{5a^5\alpha_2}{16} + a\Lambda^2\Omega^2\beta_1 \\ +9a\Lambda^4\Omega^2\beta_2 + \frac{9a^3\Lambda^2\Omega^2\beta_2}{4} + a\Lambda^2\beta_1 \\ +\frac{a^3\beta_1}{4} + 3a\Lambda^4\beta_2 + \frac{15a^3\Lambda^2\beta_2}{4} + \frac{a^5\beta_2}{4} \\ +\frac{ag_p\cos\tau_1}{2} + \frac{ag_d\sin\tau_2}{2} \end{pmatrix}^2 \\
&\quad \begin{pmatrix} -\frac{3\Lambda a^2\alpha_1}{4} - \frac{15\Lambda^3 a^2\alpha_2}{2} \\ -\frac{15\Lambda a^4\alpha_2}{16} + \frac{\Lambda a^2\Omega^2\beta_1}{4} \\ +\frac{15\Lambda^3 a^2\Omega^2\beta_2}{4} + \frac{3\Lambda a^4\Omega^2\beta_2}{16} \\ -\frac{\Lambda a^2\Omega\beta_1}{2} - \frac{3\Lambda^3 a^2\Omega\beta_2}{2} \\ -\frac{\Lambda a^4\Omega\beta_2}{8} + \frac{3\Lambda a^2\beta_1}{4} \\ +\frac{15\Lambda^3 a^2\beta_2}{4} + \frac{9\Lambda a^4\beta_2}{16} \end{pmatrix}^2
\end{aligned} \tag{43}
$$

Case 3: when $\Omega = 5 + \varepsilon\sigma$, one obtains

$$
\begin{aligned}
&-6A\Lambda^2\alpha_1 - 3A^2\bar{A}\alpha_1 - 30A\Lambda^4\alpha_2 - 60A^2\Lambda^2\bar{A}\alpha_2 \\
&-10A^3\bar{A}^2\alpha_2 + 2A\Lambda^2\Omega^2\beta_1 \\
&+18A\Lambda^4\Omega^2\beta_2 + 18A^2\Lambda^2\bar{A}\Omega^2\beta_2 - i\mu A \\
&+2A\Lambda^2\beta_1 + 2A^2\bar{A}\beta_1 + 6A\Lambda^4\beta_2 \\
&+30A^2\Lambda^2\bar{A}\beta_2 + 8A^3\bar{A}^2\beta_2 \\
&+e^{i\sigma T_1}\begin{pmatrix} -5\Lambda\bar{A}^4\alpha_2 + \Lambda\Omega^2\bar{A}^4\beta_2 - 2\Lambda\Omega\bar{A}^4\beta_2 \\ +7\Lambda\bar{A}^4\beta_2 \end{pmatrix} \\
&-2i\dot{A} + g_p A e^{-i\tau_1} + ig_d A e^{-i\tau_2} = 0
\end{aligned} \tag{44}
$$

Similarly, the frequency response equation is obtained:

$$
\begin{aligned}
&\left(-\frac{5\Lambda a^4\alpha_2}{16} + \frac{\Lambda\Omega^2 a^4\beta_2}{16} - \frac{\Lambda\Omega a^4\beta_2}{8} + \frac{7\Lambda a^4\beta_2}{16}\right)^2 \\
&= \left(\frac{\mu a}{2} + \frac{ag_p\sin\tau_1}{2} - \frac{ag_d\cos\tau_2}{2}\right)^2
\end{aligned}
$$

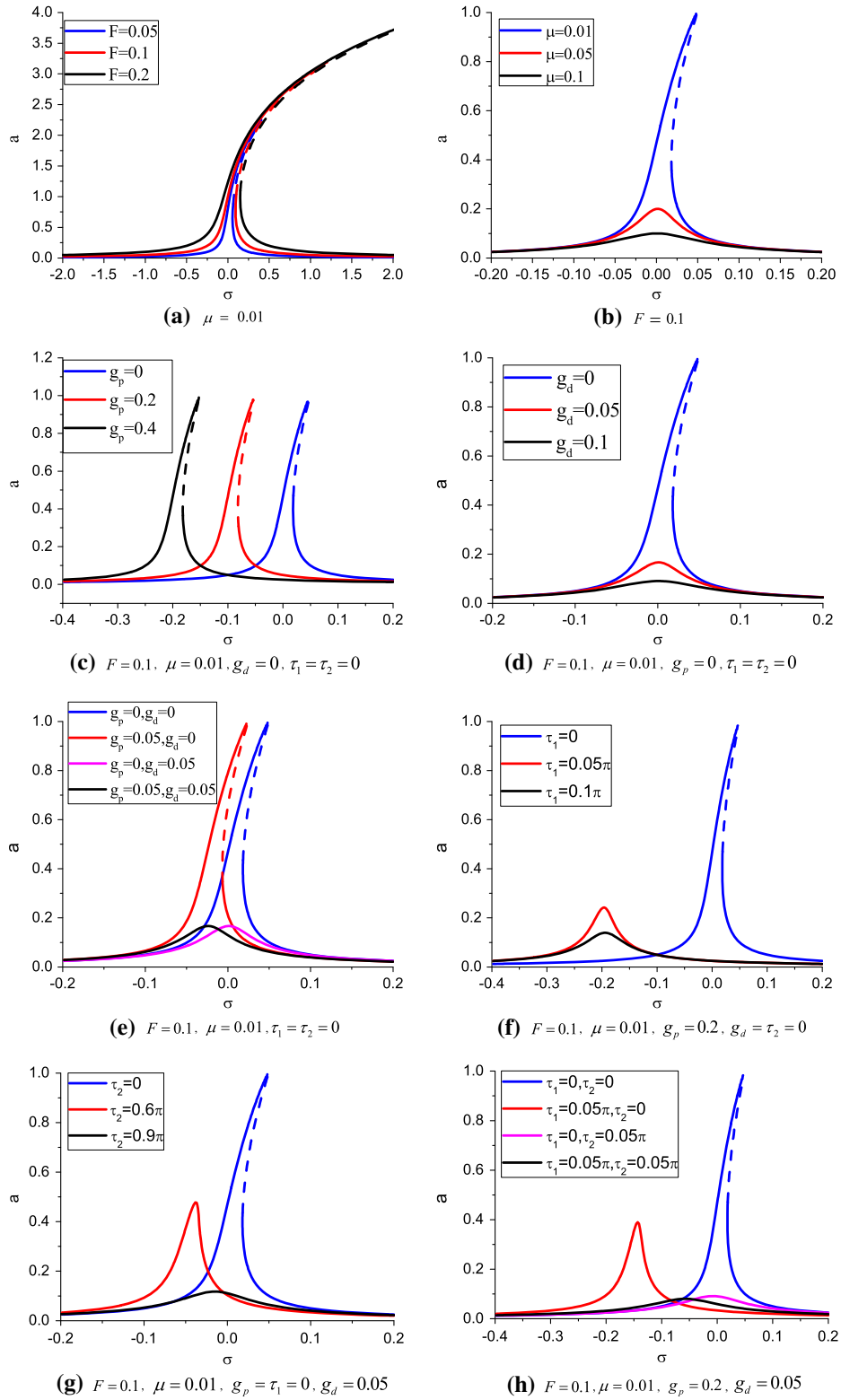


**Fig. 2** Amplitude–frequency curve of the system for the primary resonance with different delays and feedback gain coefficients

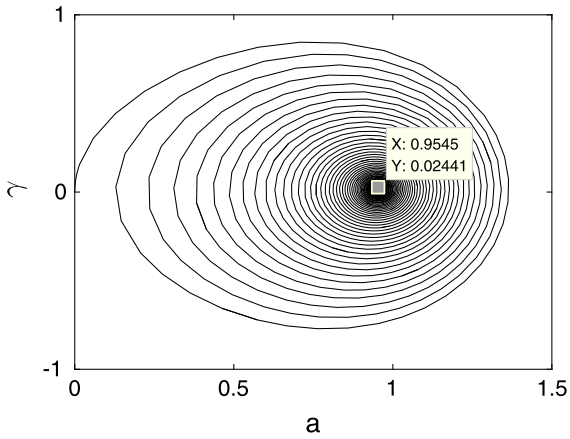


**Fig. 3** Phase–amplitude response with zero initial conditions

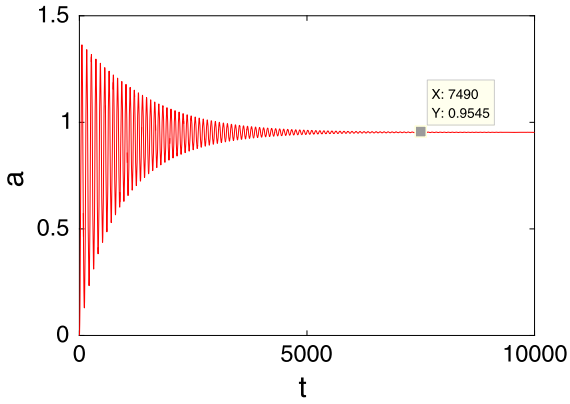


**Fig. 4** Time–amplitude response with zero initial conditions

$$+\left(\begin{array}{l}\frac{a\sigma}{5}-3a\Lambda^2\alpha_1-\frac{3a^3\alpha_1}{8}-15a\Lambda^4\alpha_2\\ -\frac{15a^3\Lambda^2\alpha_2}{2}-\frac{5a^5\alpha_2}{16}+a\Lambda^2\Omega^2\beta_1\\ +9a\Lambda^4\Omega^2\beta_2+\frac{9a^3\Lambda^2\Omega^2\beta_2}{4}+a\Lambda^2\beta_1\\ +\frac{a^3\beta_1}{4}+3a\Lambda^4\beta_2+\frac{15a^3\Lambda^2\beta_2}{4}+\frac{a^5\beta_2}{4}\\ +\frac{ag_p\cos\tau_1}{2}+\frac{ag_d\sin\tau_2}{2}\end{array}\right)^2 \quad (45)$$

## 4 Results and discussion

To investigate the nonlinear behavior of the control system (2), the primary amplitude–frequency response Eq. (17) of a cantilever beam carrying an intermediate lumped mass is considered. The influences of the feedback gain coefficients $g_p$, $g_d$ and delay feedback $\tau_1$, $\tau_2$ on the amplitude–frequency curve of the main system can be calculated with $\alpha_1 = 0.3331, \alpha_2 = 0.1299, \beta_1 = 0.3338$ and $\beta_2 = 0.1319$ [44]. In all figures of this article, a solid line indicates the stable solution, and the dashed line indicates the unstable solution. The effects of the different parameters on the primary resonance are studied, and the corresponding amplitude–frequency curves are illustrated in Fig. 2. Figure 2a, b shows the influence of the excitation amplitude and the dimensionless damping coefficient on the amplitude of the steady-state response of the system without a time delay. Obviously, the primary resonant frequency curve is shifted to the right, exhibiting hard spring and multivalued characteristics. With an increase in $F$, the response area broadens and the maximum amplitude of the vibration increases. When the damping increases, the peak amplitude decreases, the migratory nature of the resonance frequency decreases, and the curve with the characteristics of a hard spring and multivalued areas is significantly reduced. From Fig. 2a, b, we can see that the excitation amplitude has little effect on the shape of the stable resonance frequency, but the damping coefficient has an important influence on the stability behavior of the system. Obviously, the conclusions are in good agreement with Refs. [13,45]. Figure 2c shows that as the displacement feedback gain coefficient increases, the peak amplitude moves to the left, and the vibration peak amplitude, the response spring characteristic, and the stability of the system's nonlinearity do not change. However, as shown in Fig. 2d, with the increase in the velocity feedback gain coefficient, the peak amplitude obviously decreases, and it remarkably changes the stability of the system. To compare the control effects of the displacement and velocity feedback gain coefficients, different gain coefficient values are chosen, as shown in Fig. 2e.

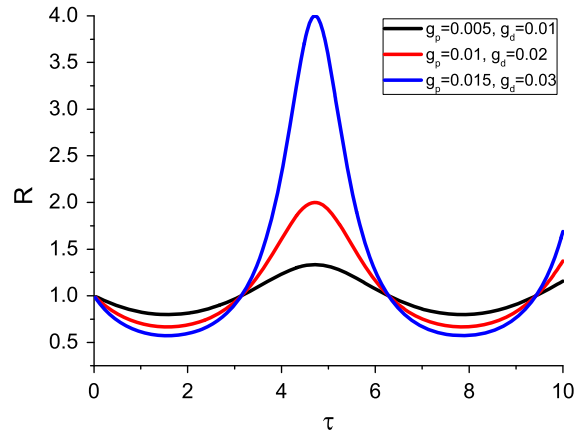


**Fig. 5** Variation of R with time delay for different feedback gain coefficients at $\mu = 0.06$ and $F = 0.1$

An increase in $g_p$ makes the peak amplitude move to a low frequency, and the increase in $g_d$ can effectively suppress the vibration amplitude of the nonlinear system. These results are consistent with those shown in Fig. 2c, d. Therefore, vibration control of a nonlinear system can be achieved by optimizing the selection of the velocity feedback gain coefficient. Figure 2f–h shows the effect of time delays on the frequency response of the system. Figure 2f, g shows that both the displacement time delay $\tau_1$ and the velocity time delay $\tau_2$ can suppress the vibration amplitude of the nonlinear system. The effectiveness of the time delay is further studied in Fig. 2h. Four cases are shown: without time delay, only displacement time delay, only velocity time delay and with two time delays. The results show that velocity delay has a more obvious effect on the nonlinear vibration of the system and that the two time delays have a better suppressive effect on system control at lower frequencies. Obviously, with the change in the time delay and feedback gain coefficient, the effect of nonlinear suppression is enhanced. It is also observed that the results of this paper agree well with those in Refs. [24–26]. Therefore, choosing an appropriate time delay and feedback gain coefficient can improve the control effect and stability of the nonlinear system. To further illustrate the validity of the results, the phase diagram and the time–amplitude response diagram are shown in Figs. 3 and 4 with zero initial conditions when $g_p = 0.01$, $g_d = 0.01$, $\tau_1 = 0.05\pi$, $\tau_2 = 0.05\pi$. It can be seen from the figures that the vibration response of the system eventually tends toward stability.

The relations between the attenuation ratio and time delay with different feedback gain coefficients are presented in Fig. 5. The figure states that reasonable selection of time delays for different feedback gain coefficients gives a small value of the attenuation rate $R$. The smaller $R$, the better vibration control of system. Obviously, $\frac{\pi}{2}$ is one of the optimal time delays.

For the superharmonic case of $\omega = \frac{1}{2}\omega_0$, the effects of $F$ and $\mu$ are illustrated in Fig. 6a, b. The only stable response for this case is zero amplitude (which is presented by a solid line), while the other curves are unstable. The effects of the feedback gain coefficient and time delay are shown in Fig. 6c–h. The results show that these parameters only have a certain influence on the system resonance bandwidth. Similarly, Figs. 7 and 8 are plotted for the superharmonic case of $\omega = \frac{1}{3}\omega_0$ and $\omega = \frac{1}{5}\omega_0$. Moreover, when $\omega \approx \frac{1}{5}\omega_0$, the control effect is more obvious. This result is consistent with the primary resonance result.

A similar parametric study is performed for all the cases ($\omega \approx 2\omega_0$, $\omega \approx 3\omega_0$ and $\omega \approx 5\omega_0$) of the subharmonic resonances, and their results are shown in Figs. 9, 10 and 11, respectively. It can be seen from the figures that each curve has two branches corresponding to two different values of the amplitude. In the two branches, the large amplitude is stable, and the small amplitude is unstable. The displacement feedback gain coefficient only makes the peak amplitude of system move to a low frequency, but the velocity feedback gain coefficient can change the amplitude and the bandwidth when subharmonic resonance occurs.

We now turn our attention to the influence of location of the concentrated mass on the primary resonance of the system. According to Ref. [44], the values of dimensionless parameters are taken as $\alpha_1 = 0.3331$, $\alpha_2 = 0.1299$, $\beta_1 = 0.1850$ and $\beta_2 = 0.4306$. The amplitude–frequency curves of the system for tip mass subjected to base excitation are plotted in Fig. 12. It is noticed that the system shows softening behavior which is different from Fig. 2. The results also reveal that the increase of displacement feedback gain coefficient only makes the peak amplitude of system move to a low frequency. Yet velocity feedback coefficient and their time delays are able to effectively restrain the amplitude of the system. Furthermore, velocity feedback coefficient is significant for the stability of the system, but the displacement feedback gain coefficient only causes a translation of stable points of the system. These results are consistent well with those in Fig. 2.

## 5 Conclusion

In this paper, we presented an analysis of the dynamics of a cantilever beam carrying an lumped mass with time-delay displacement and velocity feedback. The multiple scales method is used to approximate the primary, superharmonic and subharmonic resonance conditions of the control system and to investigate their stability. The variation of the amplitude–frequency response curve of the system under different time delays was discussed and solved numerically. The results show that the system exhibits a hard spring characteristic for a lumped mass at an intermediate position, whereas it shows softening behavior for tip mass. The delayed displacement and velocity feedback con-

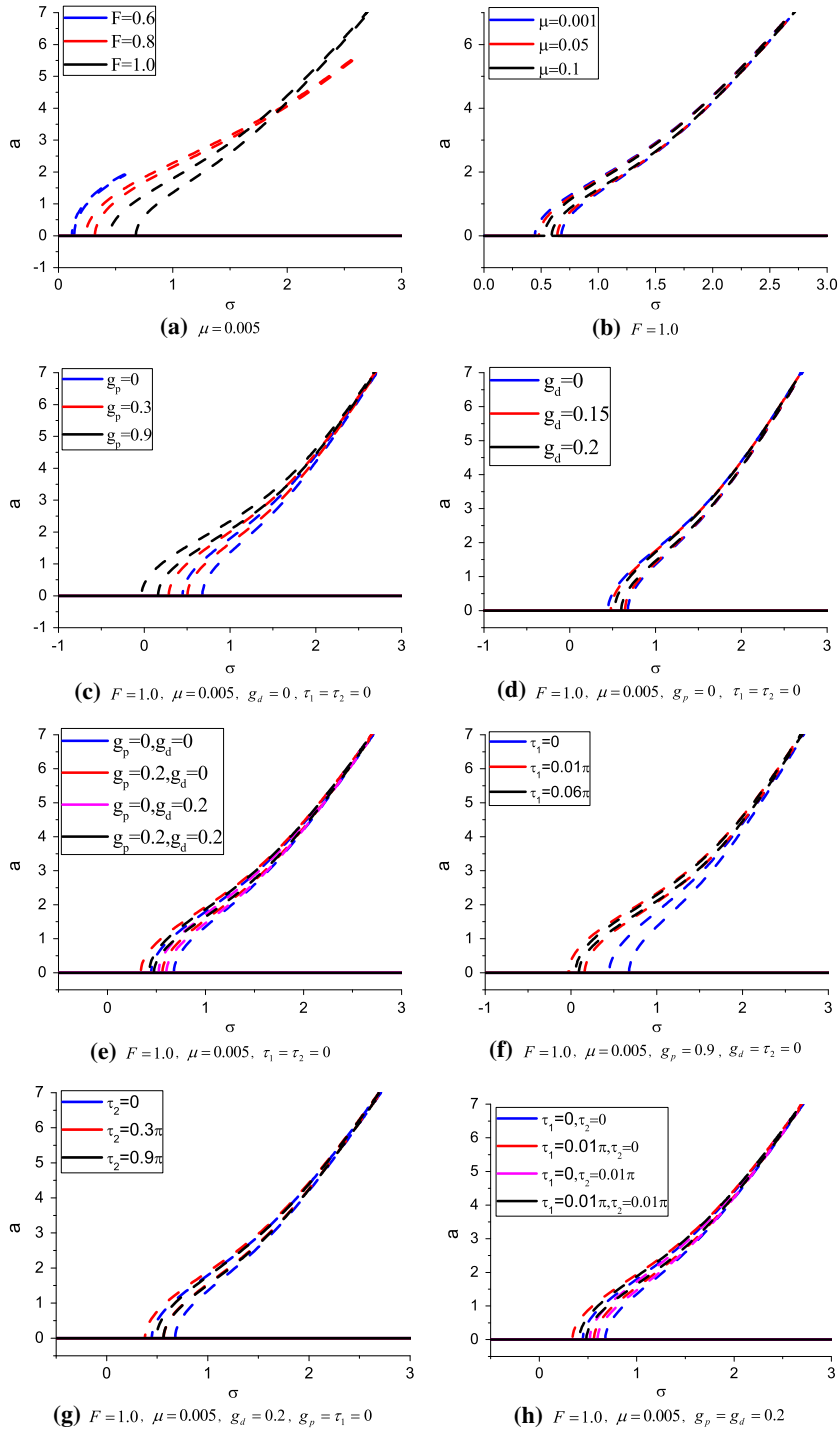


**(a)** $\mu = 0.005$ **(b)** $F = 1.0$

**(c)** $F = 1.0,\ \mu = 0.005,\ g_d = 0,\ \tau_1 = \tau_2 = 0$ **(d)** $F = 1.0,\ \mu = 0.005,\ g_p = 0,\ \tau_1 = \tau_2 = 0$

**(e)** $F = 1.0,\ \mu = 0.005,\ \tau_1 = \tau_2 = 0$ **(f)** $F = 1.0,\ \mu = 0.005,\ g_p = 0.9,\ g_d = \tau_2 = 0$

**(g)** $F = 1.0,\ \mu = 0.005,\ g_d = 0.2,\ g_p = \tau_1 = 0$ **(h)** $F = 1.0,\ \mu = 0.005,\ g_p = g_d = 0.2$

**Fig. 6** Amplitude–frequency curves of the system for the superharmonic case of $\omega \approx \frac{1}{2}\omega_0$ with different delays and feedback gain coefficients

trol terms have significant effects on the resonance stability and peak amplitude. A specific time delay control can effectively reduce the amplitude of the resonance. Moreover, by comparing the feedback gain coefficient and time delay, it is found that under the same conditions, the control effects of the velocity feedback gain coefficient and the velocity time delay are relatively good. When four control variables exist at the same time, the control effect of the system is better.

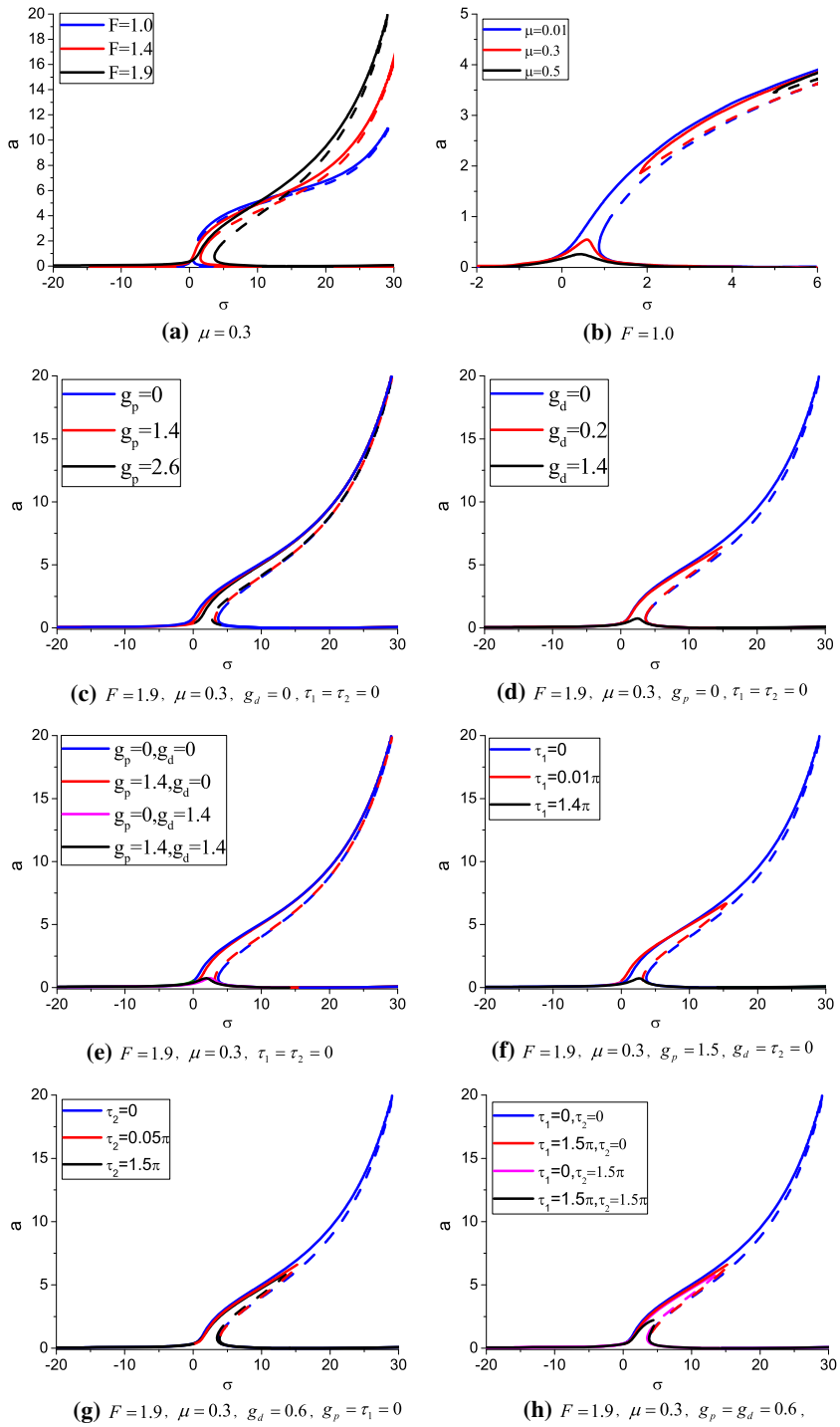


**(a)** $\mu = 0.3$ **(b)** $F = 1.0$

**(c)** $F = 1.9,\ \mu = 0.3,\ g_d = 0,\ \tau_1 = \tau_2 = 0$ **(d)** $F = 1.9,\ \mu = 0.3,\ g_p = 0,\ \tau_1 = \tau_2 = 0$

**(e)** $F = 1.9,\ \mu = 0.3,\ \tau_1 = \tau_2 = 0$ **(f)** $F = 1.9,\ \mu = 0.3,\ g_p = 1.5,\ g_d = \tau_2 = 0$

**(g)** $F = 1.9,\ \mu = 0.3,\ g_d = 0.6,\ g_p = \tau_1 = 0$ **(h)** $F = 1.9,\ \mu = 0.3,\ g_p = g_d = 0.6,$

**Fig. 7** Amplitude–frequency curves of the system for the superharmonic case of $\omega \approx \frac{1}{3}\omega_0$ with different delays and feedback gain coefficients

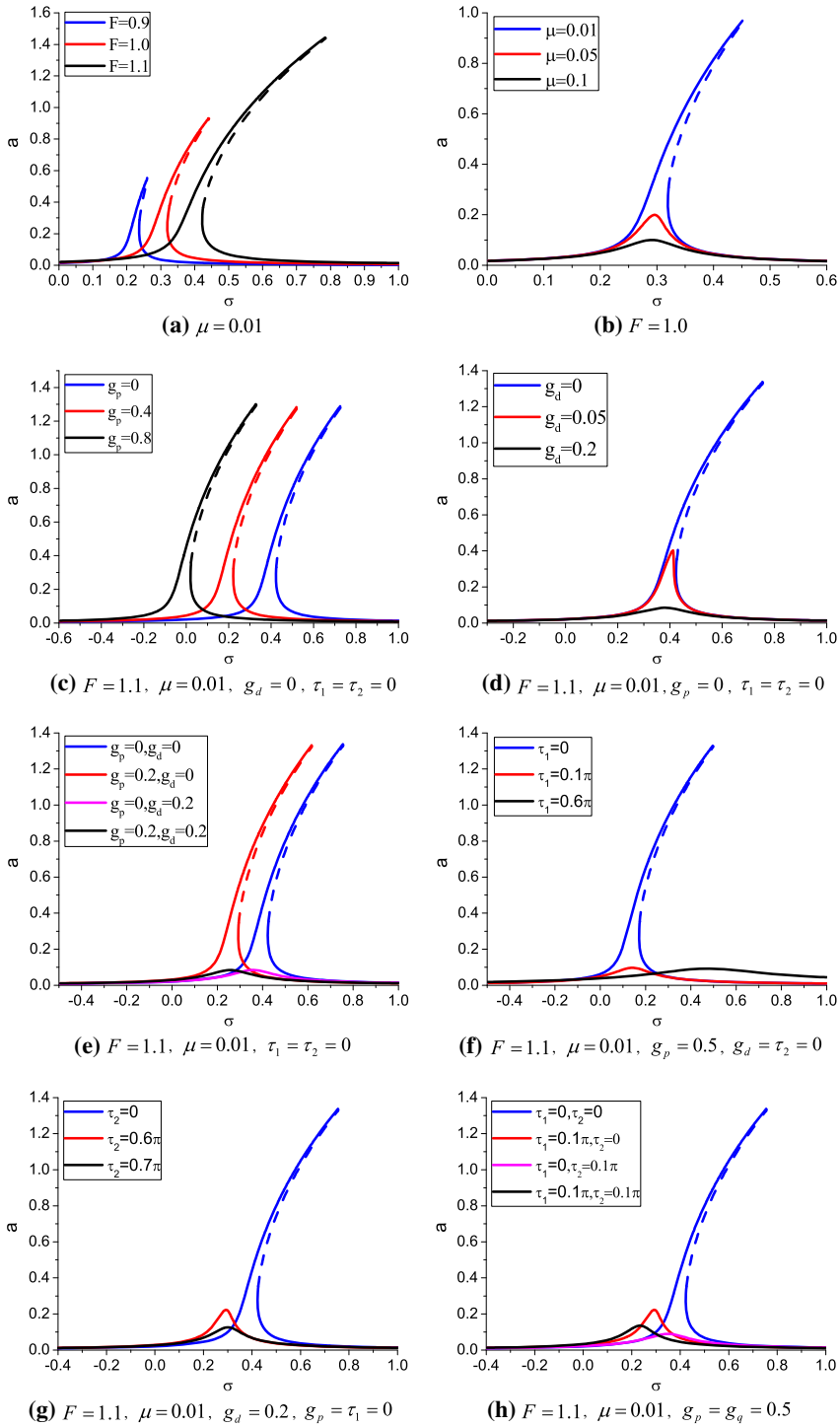


**(a)** $\mu = 0.01$ **(b)** $F = 1.0$

**(c)** $F = 1.1,\ \mu = 0.01,\ g_d = 0,\ \tau_1 = \tau_2 = 0$ **(d)** $F = 1.1,\ \mu = 0.01, g_p = 0,\ \tau_1 = \tau_2 = 0$

**(e)** $F = 1.1,\ \mu = 0.01,\ \tau_1 = \tau_2 = 0$ **(f)** $F = 1.1,\ \mu = 0.01,\ g_p = 0.5,\ g_d = \tau_2 = 0$

**(g)** $F = 1.1,\ \mu = 0.01,\ g_d = 0.2,\ g_p = \tau_1 = 0$ **(h)** $F = 1.1,\ \mu = 0.01,\ g_p = g_q = 0.5$

**Fig. 8** Amplitude–frequency curves of the system for the superharmonic case of $\omega \approx \frac{1}{5}\omega_0$ with different delays and feedback gain coefficients

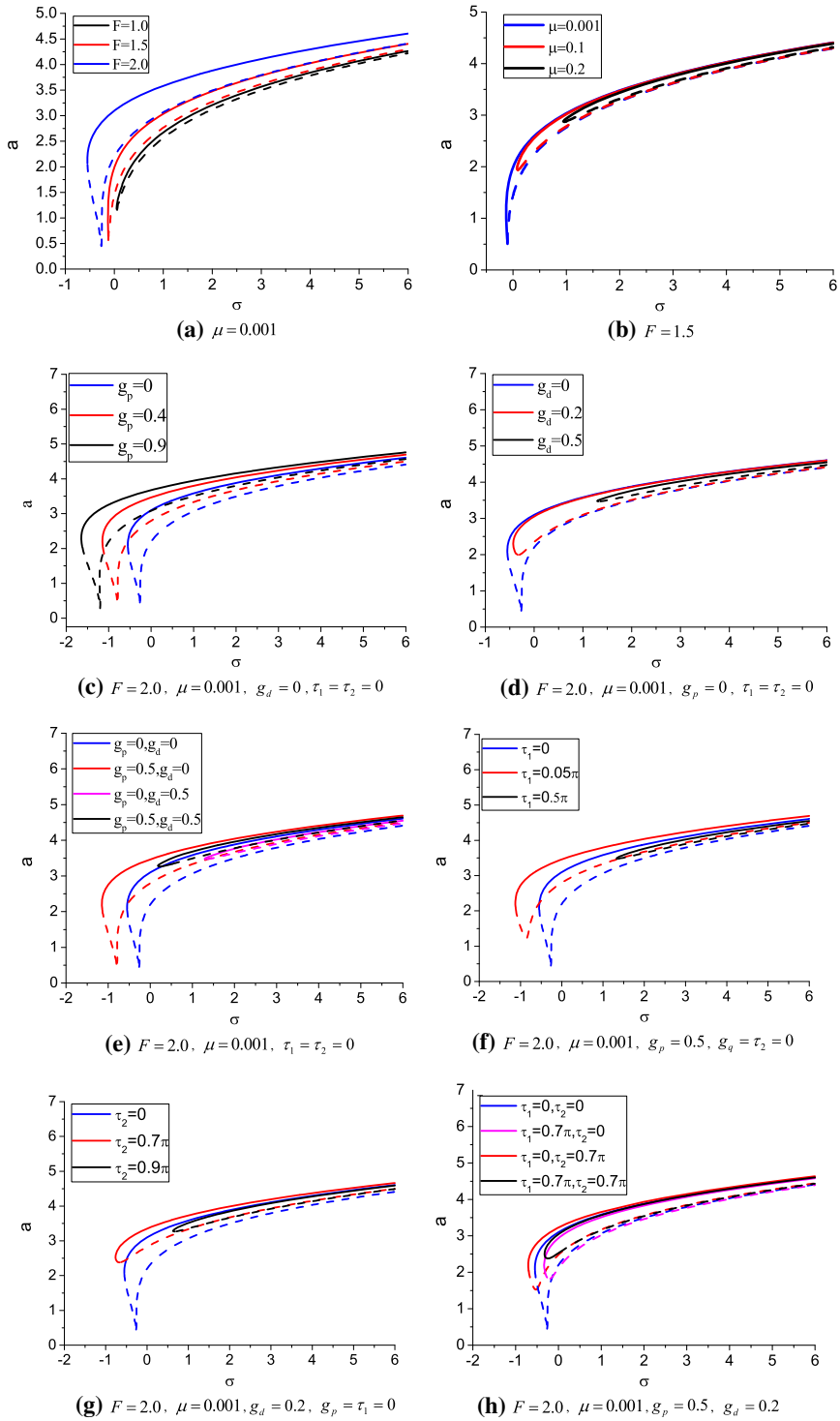


**(a)** $\mu = 0.001$ **(b)** $F = 1.5$

**(c)** $F = 2.0,\ \mu = 0.001,\ g_d = 0,\ \tau_1 = \tau_2 = 0$ **(d)** $F = 2.0,\ \mu = 0.001,\ g_p = 0,\ \tau_1 = \tau_2 = 0$

**(e)** $F = 2.0,\ \mu = 0.001,\ \tau_1 = \tau_2 = 0$ **(f)** $F = 2.0,\ \mu = 0.001,\ g_p = 0.5,\ g_q = \tau_2 = 0$

**(g)** $F = 2.0,\ \mu = 0.001, g_d = 0.2,\ g_p = \tau_1 = 0$ **(h)** $F = 2.0,\ \mu = 0.001, g_p = 0.5,\ g_d = 0.2$

**Fig. 9** Amplitude–frequency curves of the system for subharmonic case of $\omega \approx 2\omega_0$ with different delays and feedback gain coefficients

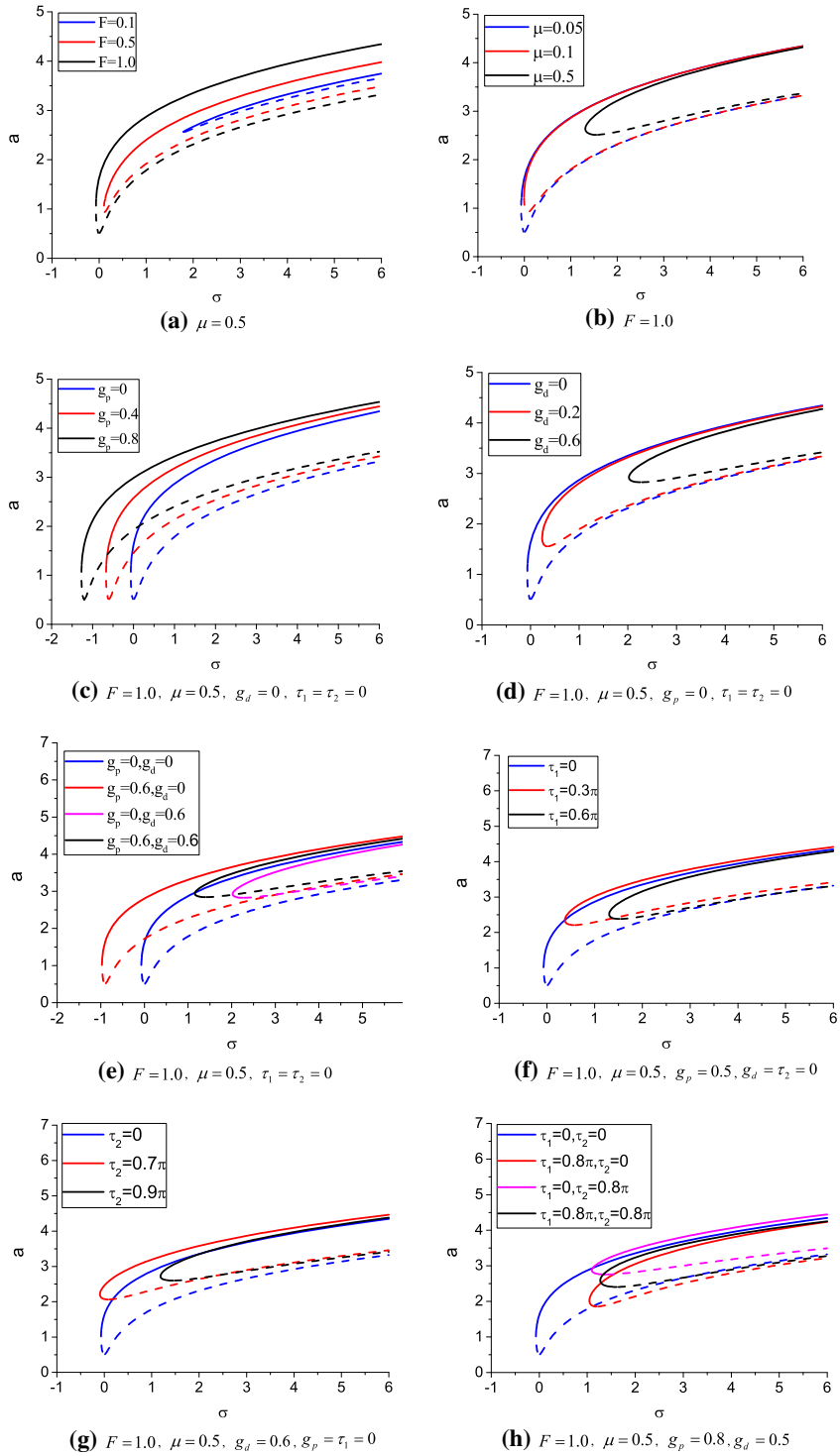


**(a)** $\mu = 0.5$ **(b)** $F = 1.0$

**(c)** $F = 1.0,\ \mu = 0.5,\ g_d = 0,\ \tau_1 = \tau_2 = 0$ **(d)** $F = 1.0,\ \mu = 0.5,\ g_p = 0,\ \tau_1 = \tau_2 = 0$

**(e)** $F = 1.0,\ \mu = 0.5,\ \tau_1 = \tau_2 = 0$ **(f)** $F = 1.0,\ \mu = 0.5,\ g_p = 0.5, g_d = \tau_2 = 0$

**(g)** $F = 1.0,\ \mu = 0.5,\ g_d = 0.6, g_p = \tau_1 = 0$ **(h)** $F = 1.0,\ \mu = 0.5,\ g_p = 0.8, g_d = 0.5$

**Fig. 10** Amplitude–frequency curves of the system for subharmonic case of $\omega \approx 3\omega_0$ with different delays and feedback gain coefficients

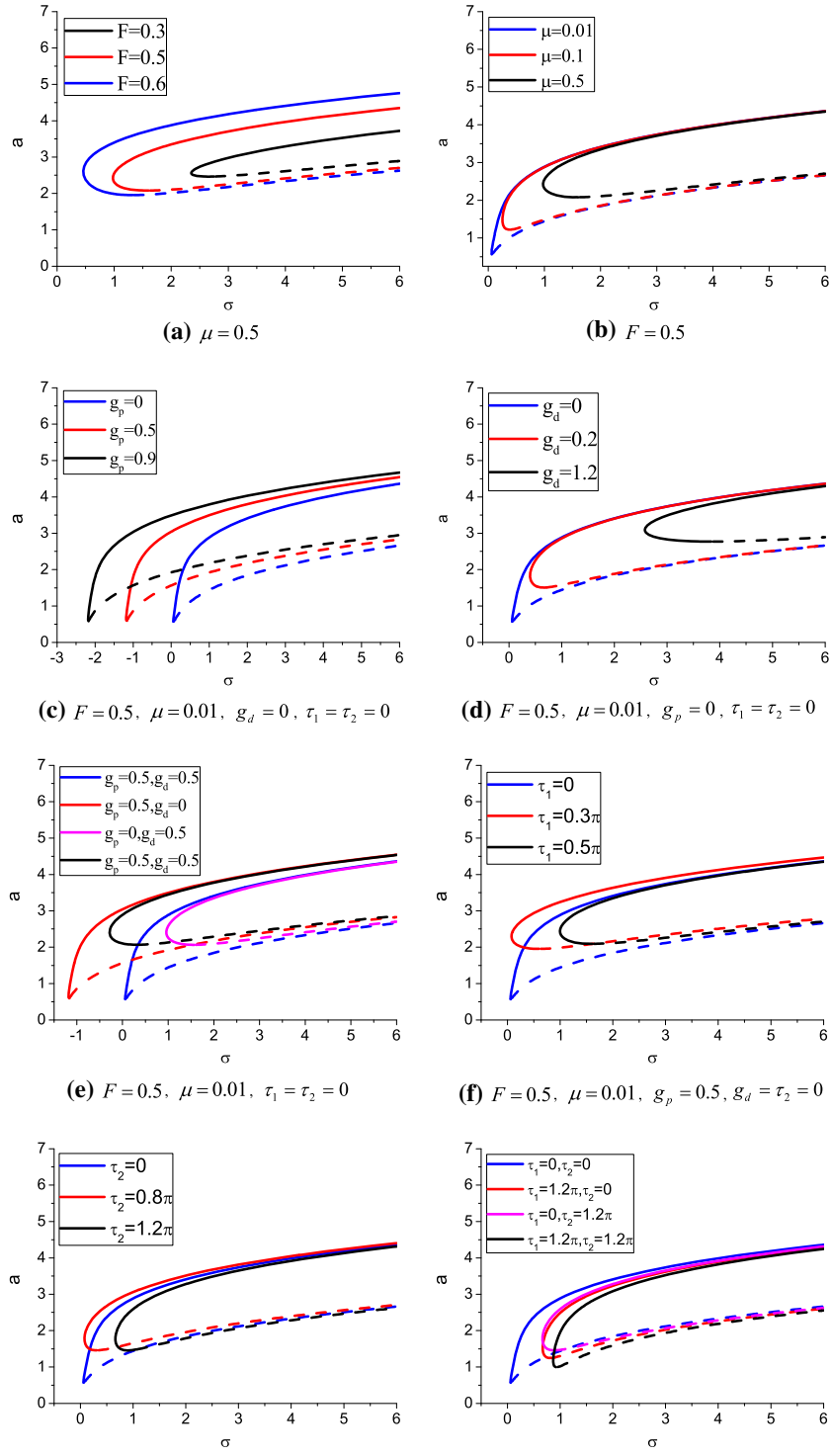


**(a)** $\mu = 0.5$ **(b)** $F = 0.5$

**(c)** $F = 0.5,\ \mu = 0.01,\ g_d = 0,\ \tau_1 = \tau_2 = 0$ **(d)** $F = 0.5,\ \mu = 0.01,\ g_p = 0,\ \tau_1 = \tau_2 = 0$

**(e)** $F = 0.5,\ \mu = 0.01,\ \tau_1 = \tau_2 = 0$ **(f)** $F = 0.5,\ \mu = 0.01,\ g_p = 0.5, g_d = \tau_2 = 0$

**(g)** $F = 0.5,\ \mu = 0.01,\ g_d = 0.2, g\ = \tau_1 = 0$ **(h)** $F = 0.5,\ \mu = 0.01,\ g_p = g_d = 0.2$

**Fig. 11** Amplitude–frequency curves of the system for subharmonic case of $\omega \approx 5\omega_0$ with different delays and feedback gain coefficients

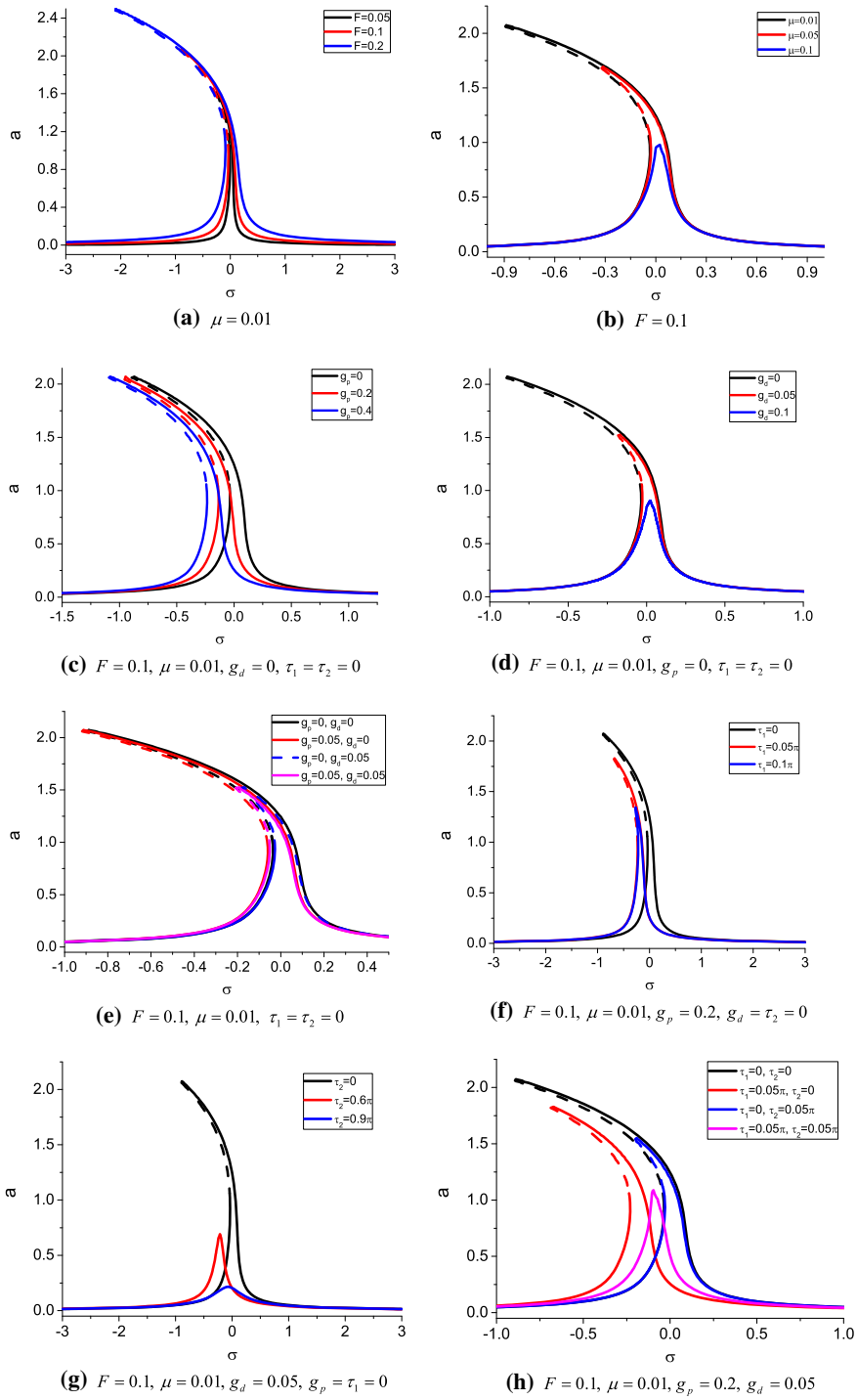


**(a)** $\mu = 0.01$ **(b)** $F = 0.1$

**(c)** $F = 0.1,\ \mu = 0.01,\ g_d = 0,\ \tau_1 = \tau_2 = 0$ **(d)** $F = 0.1,\ \mu = 0.01,\ g_p = 0,\ \tau_1 = \tau_2 = 0$

**(e)** $F = 0.1,\ \mu = 0.01,\ \tau_1 = \tau_2 = 0$ **(f)** $F = 0.1,\ \mu = 0.01,\ g_p = 0.2,\ g_d = \tau_2 = 0$

**(g)** $F = 0.1,\ \mu = 0.01,\ g_d = 0.05,\ g_p = \tau_1 = 0$ **(h)** $F = 0.1,\ \mu = 0.01,\ g_p = 0.2,\ g_d = 0.05$

**Fig. 12** Amplitude–frequency curve of the system for the primary resonance of tip mass with different delays and feedback gain coefficients

**Acknowledgements** The work described in this paper is funded by the research Grant from the Natural Science Foundation of China (Grant Nos. 11662006 and 11172115). The authors are grateful for their financial support.

**Compliance with ethical standards**

**Conflict of interest** The authors declare no conflict of interest.

## Appendix A

$$
\begin{aligned}
\varepsilon^1:\ & D_0^2 u_1 + u_1 = +e^{-5i\Omega T_0}\left(-\alpha_2\Lambda^5 + 2\Lambda^5\beta_2\Omega^2\right) \\
& + e^{5i\Omega T_0}\left(-\alpha_2\Lambda^5 + 2\Lambda^5\beta_2\Omega^2\right) + e^{-5iT_0}\left(-\alpha_2 A^5 + 2A^5\beta_2\right) \\
& + e^{5iT_0}\left(-\alpha_2 A^5 + 2A^5\beta_2\right) \\
& + e^{-3i\Omega T_0}\begin{pmatrix} -\alpha_1\Lambda^3 - 20A\bar{A}\alpha_2\Lambda^3 - 5\alpha_2\Lambda^5 + 2\beta_1\Omega^2\Lambda^3 + 12A\bar{A}\beta_2\Lambda^3\Omega^2 \\ +6\beta_2\Lambda^5\Omega^2 + 6A\bar{A}\beta_2\Lambda^3\Omega^2 + 6A\bar{A}\beta_2\Lambda^3 \end{pmatrix} \\
& + e^{3i\Omega T_0}\begin{pmatrix} -\alpha_1\Lambda^3 - 20A\bar{A}\alpha_2\Lambda^3 - 5\alpha_2\Lambda^5 + 2\beta_1\Omega^2\Lambda^3 + 12A\bar{A}\beta_2\Lambda^3\Omega^2 \\ +6\beta_2\Lambda^5\Omega^2 + 6A\bar{A}\beta_2\Lambda^3\Omega^2 + 6A\bar{A}\beta_2\Lambda^3 \end{pmatrix} \\
& + e^{-i\Omega T_0}\begin{pmatrix} -6A\bar{A}\alpha_1\Lambda - 30A^2\bar{A}^2\alpha_2\Lambda - 3\alpha_1\Lambda^3 - 60A\bar{A}\alpha_2\Lambda^3 - 10\alpha_2\Lambda^5 \\ +2A\bar{A}\beta_1\Lambda\Omega^2 + 2\beta_1\Lambda^3\Omega^2 + 6A^2\bar{A}^2\beta_2\Lambda\Omega^2 + 30A\bar{A}\beta_2\Lambda^3\Omega^2 \\ +8\beta_2\Lambda^5\Omega^2 + 2A\bar{A}\beta_1\Lambda + 18A^2\bar{A}^2\beta_2\Lambda + 18A\bar{A}\beta_2\Lambda^3 \end{pmatrix} \\
& + e^{i\Omega T_0}\begin{pmatrix} -6A\bar{A}\alpha_1\Lambda - 30A^2\bar{A}^2\alpha_2\Lambda - 3\alpha_1\Lambda^3 - 60A\bar{A}\alpha_2\Lambda^3 - 10\alpha_2\Lambda^5 \\ +2A\bar{A}\beta_1\Lambda\Omega^2 + 2\beta_1\Lambda^3\Omega^2 + 6A^2\bar{A}^2\beta_2\Lambda\Omega^2 + 30A\bar{A}\beta_2\Lambda^3\Omega^2 \\ +8\beta_2\Lambda^5\Omega^2 + 2A\bar{A}\beta_1\Lambda + 18A^2\bar{A}^2\beta_2\Lambda + 18A\bar{A}\beta_2\Lambda^3 \end{pmatrix} \\
& + e^{4iT_0}\begin{pmatrix} e^{i\Omega T_0}\left(-5A^4\alpha_2\Lambda + A^4\beta_2\Lambda\Omega^2 + 2A^4\beta_2\Lambda\Omega + 7A^4\beta_2\Lambda\right) \\ +e^{-i\Omega T_0}\left(-5A^4\alpha_2\Lambda + A^4\beta_2\Lambda\Omega^2 - 2A^4\beta_2\Lambda\Omega + 7A^4\beta_2\Lambda\right) \end{pmatrix} \\
& + e^{-4iT_0}\begin{pmatrix} e^{i\Omega T_0}\left(-5A^4\alpha_2\Lambda + A^4\beta_2\Lambda\Omega^2 + 2A^4\beta_2\Lambda\Omega + 7A^4\beta_2\Lambda\right) \\ +e^{-i\Omega T_0}\left(-5A^4\alpha_2\Lambda + A^4\beta_2\Lambda\Omega^2 - 2A^4\beta_2\Lambda\Omega + 7A^4\beta_2\Lambda\right) \end{pmatrix} \\
& + e^{3iT_0}\begin{pmatrix} -A^3\alpha_1 - 5A^4\bar{A}\alpha_2 - 20A^3\alpha_2\Lambda^2 + 6A^3\beta_2\Lambda^2\Omega^2 + 2A^3\beta_1 + 6A^4\bar{A}\beta_2 \\ +18A^3\beta_2\Lambda^2 \\ +e^{2i\Omega T_0}\left(-10A^3\alpha_2\Lambda^2 + 5A^3\Lambda^2\beta_2\Omega^2 + 6A^3\beta_2\Lambda^2\Omega + 9A^3\beta_2\Lambda^2\right) \\ +e^{-2i\Omega T_0}\left(-10A^3\alpha_2\Lambda^2 + 5A^3\Lambda^2\beta_2\Omega^2 - 6A^3\beta_2\Lambda^2\Omega + 9A^3\beta_2\Lambda^2\right) \end{pmatrix} \\
& + e^{-3iT_0}\begin{pmatrix} -A^3\alpha_1 - 5A^4\bar{A}\alpha_2 - 20A^3\alpha_2\Lambda^2 + 6A^3\beta_2\Lambda^2\Omega^2 + 2A^3\beta_1 + 6A^4\bar{A}\beta_2 \\ +18A^3\beta_2\Lambda^2 \\ +e^{2i\Omega T_0}\left(-10A^3\alpha_2\Lambda^2 + 5A^3\Lambda^2\beta_2\Omega^2 + 6A^3\beta_2\Lambda^2\Omega + 9A^3\beta_2\Lambda^2\right) \\ +e^{-2i\Omega T_0}\left(-10A^3\alpha_2\Lambda^2 + 5A^3\Lambda^2\beta_2\Omega^2 - 6A^3\beta_2\Lambda^2\Omega + 9A^3\beta_2\Lambda^2\right) \end{pmatrix} \\
& + e^{iT_0}\begin{pmatrix} -3A^2\alpha_1\bar{A} - 10A^3\bar{A}^2\alpha_2 - 6A\alpha_1\Lambda^2 - 60A^2\bar{A}\alpha_2\Lambda^2 - 30A\alpha_2\Lambda^4 + 2A\Lambda^2\beta_1\Omega^2 \\ +18A^2\bar{A}\Lambda^2\beta_2\Omega^2 + 18A\Lambda^4\beta_2\Omega^2 + 2A^2\bar{A}\beta_1 + 2A\Lambda^2\beta_1 + 8A^3\bar{A}^2\beta_2 \\ +30A^2\bar{A}\Lambda^2\beta_2\omega_0^2 + 6A\Lambda^4\beta_2 + g_p A e^{-i\tau_1} + i g_d A e^{-i\tau_2} \\ +e^{4i\Omega T_0}\left(-5A\alpha_2\Lambda^4 + 7A\Lambda^4\beta_2\Omega^2 + 2A\beta_2\Lambda^4\Omega + A\beta_2\Lambda^4\right) \\ +e^{-4i\Omega T_0}\left(-5A\alpha_2\Lambda^4 + 7A\Lambda^4\beta_2\Omega^2 - 2A\beta_2\Lambda^4\Omega + A\beta_2\Lambda^4\right) \end{pmatrix} \\
& + e^{iT_0}e^{2i\Omega T_0}\begin{pmatrix} -3A\alpha_1\Lambda^2 - 30A^2\bar{A}\alpha_2\Lambda^2 - 20A\alpha_2\Lambda^4 + 3A\Lambda^2\beta_1\Omega^2 + 15A^2\bar{A}\Lambda^2\beta_2\Omega^2 \\ 16A\Lambda^4\beta_2\Omega^2 + 2A\Lambda^2\beta_1\Omega + 6A^2\bar{A}\Lambda^2\beta_2\Omega + 4A\Lambda^4\beta_2\Omega + A\Lambda^2\beta_1 \\ +15A^2\bar{A}\Lambda^2\beta_2 + 4A\Lambda^4\beta_2 \end{pmatrix}
\end{aligned}
$$

$$
\begin{aligned}
&+\ e^{iT_0}e^{-2i\Omega T_0}\begin{pmatrix}-3A\alpha_1\Lambda^2-30A^2\bar{A}\alpha_2\Lambda^2-20A\alpha_2\Lambda^4+3A\Lambda^2\beta_1\Omega^2+15A^2\bar{A}\Lambda^2\beta_2\Omega^2\\16A\Lambda^4\beta_2\Omega^2-2A\Lambda^2\beta_1\Omega-6A^2\bar{A}\Lambda^2\beta_2\Omega-4A\Lambda^4\beta_2\Omega+A\Lambda^2\beta_1\\+15A^2\bar{A}\Lambda^2\beta_2+4A\Lambda^4\beta_2\end{pmatrix}\\
&+\ e^{-iT_0}\begin{pmatrix}-3A^2\alpha_1\bar{A}-10A^3\bar{A}^2\alpha_2-6A\alpha_1\Lambda^2-60A^2\bar{A}\alpha_2\Lambda^2-30A\alpha_2\Lambda^4\\+2A\Lambda^2\beta_1\Omega^2+18A^2\bar{A}\Lambda^2\beta_2\Omega^2+18A\Lambda^4\beta_2\Omega^2+2A^2\bar{A}\beta_1\\+2A\Lambda^2\beta_1+8A^3\bar{A}^2\beta_2+30A^2\bar{A}\Lambda^2\beta_2+6A\Lambda^4\beta_2\\+e^{4i\Omega T_0}\left(-5A\alpha_2\Lambda^4+7A\Lambda^4\beta_2\Omega^2+2A\beta_2\Lambda^4\Omega+A\beta_2\Lambda^4\right)\\+e^{-4i\Omega T_0}\left(-5A\alpha_2\Lambda^4+7A\Lambda^4\beta_2\Omega^2-2A\beta_2\Lambda^4\Omega+A\beta_2\Lambda^4\right)\end{pmatrix}\\
&+\ e^{-iT_0}e^{2i\Omega T_0}\begin{pmatrix}-3A\alpha_1\Lambda^2-30A^2\bar{A}\alpha_2\Lambda^2-20A\alpha_2\Lambda^4+3A\Lambda^2\beta_1\Omega^2\\+15A^2\bar{A}\Lambda^2\beta_2\Omega^2+16A\Lambda^4\beta_2\Omega^2+2A\Lambda^2\beta_1\Omega\\+6A^2\bar{A}\Lambda^2\beta_2\Omega+4A\Lambda^4\beta_2\Omega+A\Lambda^2\beta_1\\+15A^2\bar{A}\Lambda^2\beta_2+4A\Lambda^4\beta_2\end{pmatrix}\\
&+\ e^{-iT_0}e^{-2i\Omega T_0}\begin{pmatrix}-3A\alpha_1\Lambda^2-30A^2\bar{A}\alpha_2\Lambda^2-20A\alpha_2\Lambda^4+3A\Lambda^2\beta_1\Omega^2\\+15A^2\bar{A}\Lambda^2\beta_2\Omega^2+16A\Lambda^4\beta_2\Omega^2-2A\Lambda^2\beta_1\Omega\\-6A^2\bar{A}\Lambda^2\beta_2\Omega-4A\Lambda^4\beta_2\Omega+A\Lambda^2\beta_1\\+15A^2\bar{A}\Lambda^2\beta_2+4A\Lambda^4\beta_2\end{pmatrix}\\
&+\ e^{2iT_0}\begin{pmatrix}e^{i\Omega T_0}\begin{pmatrix}-3A^2\alpha_1\Lambda-20A^3\bar{A}\alpha_2\Lambda-30A^2\alpha_2\Lambda^3+A^2\beta_1\Lambda\Omega^2+4A^3\bar{A}\beta_2\Lambda\Omega^2\\+15A^2\Lambda^3\beta_2\Omega^2+2A^2\beta_1\Lambda\Omega+4A^3\bar{A}\beta_2\Lambda\Omega+6A^2\Lambda^3\beta_2\Omega\\+3A^2\beta_1\Lambda+16A^3\bar{A}\beta_2\Lambda+15A^2\beta_2\Lambda^3\end{pmatrix}\\+e^{-i\Omega T_0}\begin{pmatrix}-3A^2\alpha_1\Lambda-20A^3\bar{A}\alpha_2\Lambda-30A^2\alpha_2\Lambda^3+A^2\beta_1\Lambda\Omega^2+4A^3\bar{A}\beta_2\Lambda\Omega^2\\+15A^2\Lambda^3\beta_2\Omega^2-2A^2\beta_1\Lambda\Omega-4A^3\bar{A}\beta_2\Lambda\Omega-6A^2\Lambda^3\beta_2\Omega\\+3A^2\beta_1\Lambda+16A^3\bar{A}\beta_2\Lambda+15A^2\beta_2\Lambda^3\end{pmatrix}\\+e^{3i\Omega T_0}\left(-10A^2\alpha_2\Lambda^3+9A^2\Lambda^3\beta_2\Omega^2+6A^2\Lambda^3\beta_2\Omega+5A^2\Lambda^3\beta_2\right)\\+e^{-3i\Omega T_0}\left(-10A^2\alpha_2\Lambda^3+9A^2\Lambda^3\beta_2\Omega^2-6A^2\Lambda^3\beta_2\Omega+5A^2\Lambda^3\beta_2\right)\end{pmatrix}\\
&+\ e^{-2iT_0}\begin{pmatrix}e^{i\Omega T_0}\begin{pmatrix}-3A^2\alpha_1\Lambda-20A^3\bar{A}\alpha_2\Lambda-30A^2\alpha_2\Lambda^3+A^2\beta_1\Lambda\Omega^2+4A^3\bar{A}\beta_2\Lambda\Omega^2\\+15A^2\Lambda^3\beta_2\Omega^2+2A^2\beta_1\Lambda\Omega+4A^3\bar{A}\beta_2\Lambda\Omega+6A^2\Lambda^3\beta_2\Omega\\+3A^2\beta_1\Lambda+16A^3\bar{A}\beta_2\Lambda+15A^2\beta_2\Lambda^3\end{pmatrix}\\+e^{-i\Omega T_0}\begin{pmatrix}-3A^2\alpha_1\Lambda-20A^3\bar{A}\alpha_2\Lambda-30A^2\alpha_2\Lambda^3+A^2\beta_1\Lambda\Omega^2+4A^3\bar{A}\beta_2\Lambda\Omega^2\\+15A^2\Lambda^3\beta_2\Omega^2-2A^2\beta_1\Lambda\Omega-4A^3\bar{A}\beta_2\Lambda\Omega-6A^2\Lambda^3\beta_2\Omega\\+3A^2\beta_1\Lambda+16A^3\bar{A}\beta_2\Lambda+15A^2\beta_2\Lambda^3\end{pmatrix}\\+e^{3i\Omega T_0}\left(-10A^2\alpha_2\Lambda^3+9A^2\Lambda^3\beta_2\Omega^2+6A^2\Lambda^3\beta_2\Omega+5A^2\Lambda^3\beta_2\right)\\+e^{-3i\Omega T_0}\left(-10A^2\alpha_2\Lambda^3+9A^2\Lambda^3\beta_2\Omega^2-6A^2\Lambda^3\beta_2\Omega+5A^2\Lambda^3\beta_2\right)\end{pmatrix}
\end{aligned}
\tag{32}
$$

## References


1. Kevin, M.H., Earl, D.: Nonlinear responses of inextensible cantilever and free-free beams undergoing large deflections. J. Appl. Mech. **85**(5), 051008 (2018)
2. Dwivedy, S.K., Kar, R.C.: Nonlinear dynamics of a cantilever beam carrying an attached mass with 1:3:9 internal resonances. Nonlinear Dyn. **31**(1), 49–72 (2003)
3. Kar, R.C., Dwivedy, S.K.: Non-linear dynamics of a slender beam carrying a lumped mass with principal parametric and internal resonances. Int. J. Nonlinear Mech. **34**(3), 515–529 (1999)
4. Navadeh, N., Hewson, R.W., Fallah, A.S.: Dynamics of transversally vibrating non-prism Timoshenko cantilever beams. Eng. Struct. **166**, 511–525 (2018)
5. Pratiher, B., Bhowmick, S.: Nonlinear dynamic analysis of a Cartesian manipulator carrying an end effector placed at an intermediate position. Nonlinear Dyn. **69**(1–2), 539–553 (2012)
6. Ercoli, L., Laura, P.A.A.: Analytical and experimental investigation on continuous beams carrying elastically mounted masses. J. Sound Vib. **114**, 519–533 (1987)
7. Gürgöze, M.: On the eigen-frequencies of a cantilever beam with attached tip mass and a spring-mass system. J. Sound Vib. **190**(2), 149–162 (1996)
8. Kanaka, R.K., Venkateswara, R.G.: Towards improved evaluation of large amplitude free-vibration behaviour of uniform beams using multi-term admissible functions. J. Sound Vib. **282**, 1238–1246 (2005)
9. Kazemi-Lari, M.A., Fazelzadeh, S.A.: Flexural-torsional flutter analysis of a deep cantilever beam subjected to a partially distributed lateral force. Acta Mech. **226**(5), 1379–1393 (2015)
10. Rhoads, J.F., Shaw, S.W., Turner, K.L.: The nonlinear response of resonant microbeam systems with purely parametric electrostatic actuation. J. Micromech. Microeng. **16**, 890–899 (2006)
11. Nayfeh, A.H., Younis, M.I.: Dynamics of MEMS resonators under superharmonic and subharmonic excitations. J. Micromech. Microeng. **15**, 1840–1847 (2005)
12. Ekici, H., Boyaci, H.: Effects of non-ideal boundary conditions on vibrations of microbeams. J. Vib. Control **13**(9–10), 1369–1378 (2007)
13. Mehran, S., Davood, Y., Ebrahim, E.: Nonlinear harmonic vibration and stability analysis of a cantilever beam carrying an intermediate lumped mass. Nonlinear Dyn. **84**, 1667–1682 (2016)
14. Eftekhari, S.A., Bakhtiari-Nejad, F., Dowell, E.H.: An investigation on the sensitivity of limit cycle oscillations for detecting damage in an aeroelastic panel. Appl. Mech. Mater. **110–116**, 4424–4432 (2012)
15. Eftekhari, S.A., Bakhtiari-Nejad, F., Dowell, E.H.: Damage detection of an aeroelastic panel using limit cycle oscillation analysis. J. Non-Linear Mech. **58**, 99–110 (2014)
16. Oveissi, S., Toghraie, D., Ali Eftekhari, S.: Investigation the effect of axially moving carbon nanotube and nano-flow on the vibrational behavior of the system. Int. J. Fluid Mech. Res. **45**(2), 171–186 (2018)
17. Toghraie, D., Ali Eftekhari, S., Oveissi, S.: Analysis of transverse vibration and instabilities of the axially moving carbon nanotube conveying fluid. Int. J. Fluid Mech. Res. **44**(2), 115–129 (2017)
18. Nayfeh, A.H., Younis, M.I.: Dynamics of MEMS resonators under super-harmonic and sub-harmonic excitations. J. Micromech. Microeng. **15**, 1840–1847 (2005)
19. Younis, M.I., Nayfeh, A.H.: A study of the nonlinear response of a resonant micro-beam to an electric actuation. Nonlinear Dyn. **31**, 91–117 (2003)
20. Eftekhari, M., Ziaei-Rad, S., Mahzoon, M.: Vibration suppression of a symmetrically cantilever composite beam using internal resonance under chord wise base excitation. Int. J. Non-Linear Mech. **48**, 86–100 (2013)
21. Abdel-Rahman, E.M., Younis, M.I., Nayfeh, A.H.: Characterization of the mechanical behavior of an electrically actuated micro-beam. J. Micromech. Microeng. **12**, 759–766 (2002)
22. Kuang, J.H., Chen, C.J.: Dynamic characteristics of shaped micro-actuators solved using the differential quadrature method. J. Micromech. Microeng. **14**, 647–655 (2004)
23. Amer, Y.A., El-Sayed, A.T., El-Bahrawy, F.T.: Torsional vibration reduction for rolling mill's main drive system via negative velocity feedback under parametric excitation. J. Mech. Sci. Technol. **29**(4), 1581–1589 (2015)
24. Khaled, A., Majed, A.: Free vibrations control of a cantilever beam using combined time delay feedback. J. Vib. Control **18**(5), 609–621 (2011)
25. Seyed, H.M., Amir, M.K., Amir, H.G.: Optimizing time delay feedback for active vibration control of a cantilever beam using a genetic algorithm. J. Vib. Control **22**(19), 4047–4061 (2016)
26. Cai, G.P., Yang, S.X.: A Discrete optimal control method for a flexible cantilever beam with time delay. J. Vib. Control **12**(5), 509–526 (2006)
27. Mustafa, Y.: Direct and parametric excitation of a nonlinear cantilever beam of varying orientation with time delay state feedback. J. Sound Vib. **324**, 892–902 (2009)
28. Hu, H., Dowell, E.H., Virgin, L.N.: Resonances of a harmonically forced Duffing oscillator with time delay state feedback. Nonlinear Dyn. **15**, 311 (1998)
29. Hu, H.Y., Wang, Z.H.: Nonlinear dynamics of controlled mechanical systems with time delays. Prog. Nat. Sci. **10**, 801 (2000)
30. Amer, Y.A., El-Sayed, A.T., Kotb, A.A.: Nonlinear vibration and of the Duffing oscillator to parametric excitation with time delay feedback. Nonlinear Dyn. **85**(4), 2497–2505 (2016)
31. Kirrou, I., Belhaq, M.: On the quasi-periodic response in the delayed forced Duffing oscillator. Nonlinear Dyn. **84**, 2069–2078 (2016)
32. El-Gohary, H.A., El-Ganaini, W.A.: Vibration suppression of a dynamical system to multi-parametric excitations via time-delay absorber. Appl. Math. Model. **36**, 35–45 (2012)
33. Saeed, N.A., El-Ganini, W.A., Eissa, M.: Nonlinear time delay saturation-based controller for suppression of nonlinear beam vibrations. Appl. Math. Model. **37**, 8846–8864 (2013)
34. Zhang, L., Huang, L., Zhang, Z.: Stability and Hopf bifurcation of the maglev system with delayed position and speed feedback control. Nonlinear Dyn. **57**, 197–207 (2009)
35. Wang, H., Li, J., Zhang, K.: Non-resonant response, bifurcation and oscillation suppression of a non-autonomous sys-

tem with delayed position feedback control. Nonlinear Dyn. **51**, 447–464 (2008)
36. Zhao, Y.Y., Xu, J.: Using the delayed feedback control and saturation control to suppress the vibration of the dynamical system. Nonlinear Dyn. **67**, 735–753 (2012)
37. Daqaq, M.F., Alhazza, K.A., Qaroush, Y.: On primary resonances of weakly nonlinear delay systems with cubic nonlinearities. Nonlinear Dyn. **64**, 253–277 (2011)
38. Alhazza, K.A., Daqaq, M.F., Nayfeh, A.H., Inman, D.J.: Nonlinear vibrations of parametrically excited cantilever beams subjected to non-linear delayed-feedback control. Int. J. Non-Linear Mech. **43**, 801–812 (2008)
39. Alhazza, K.A., Nayfeh, A.H., Daqaq, M.F.: On utilizing delayed feedback for active-multimode vibration control of cantilever beams. J. Sound Vib. **319**, 735–752 (2009)
40. Alhazza, K.A., Majeed, M.A.: Free vibrations control of a cantilever beam using combined time delay feedback. J. Vib. Control. **18**(5), 609–621 (2011)
41. Daqaq, M.F., Alhazza, K.A., Arafat, H.N.: Non-linear vibrations of cantilever beams with feedback delays. Int. J. Non-Linear Mech. **43**, 962–978 (2008)
42. Ji, J.C.J., Zhang, N.: Suppression of the primary resonance vibrations of a forced nonlinear system using a dynamic vibration absorber. J. Sound Vib. **329**, 2044–2056 (2010)
43. Ji, J.C., Leung, A.Y.T.: Resonances of a non-linear sdof system with two time-delays in linear feedback contror. J. Sound Vib. **253**(5), 985–1000 (2002)
44. Hamdan, M.N., Shabaneh, N.H.: On the large amplitude free vibrations of a restrained uniform beam carrying an intermediate lumped mass. J. Sound Vib. **199**(5), 711–736 (1997)
45. Xu, J., Pei, L.J.: Advances in dynamics for delayed systems. Adv. Mech. **36**, 17–30 (2006)